

AD-A100 633

MAR INC ROCKVILLE MD
VERY LOW FREQUENCY TRANSMISSION LOSS IN SHALLOW WATER. (U)
MAY 81 R H FERRIS

F/6 20/1

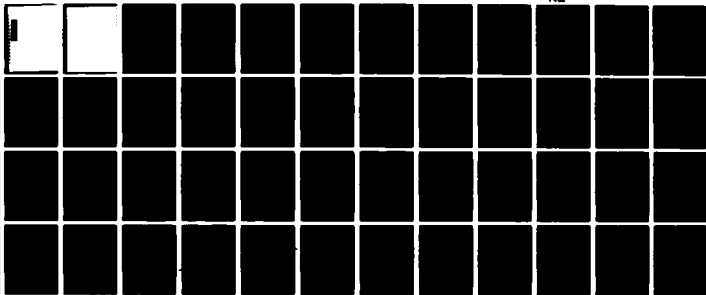
N00014-81-C-0164

NL

UNCLASSIFIED

MAR-TR-263

1000
4000
20000 40000



END
DATE
PUBLISHED
7 81
DTIC



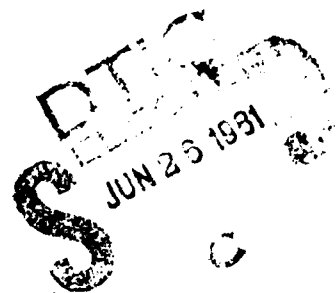
MAR. INCORPORATED
1335 ROCKVILLE PIKE
ROCKVILLE, MARYLAND 20852
AREA CODE 301
424-1310

12

VERY LOW FREQUENCY TRANSMISSION LOSS
IN SHALLOW WATER

Raymond H. Ferris

May 1981
Technical Report No. 263
Contract No. N00014-81-C-0164



OFFICE OF NAVAL RESEARCH
Arlington, Virginia 22202

APPROVED FOR PUBLIC RELEASE: DISTRIBUTION UNLIMITED

Satellite Office
2531 South Jefferson Davis Highway
Room 3N30 - Building 3
Arlington, Virginia 22202

UNCLASSIFIED

SECURITY CLASSIFICATION OF THIS PAGE (When Data Entered)

REPORT DOCUMENTATION PAGE		READ INSTRUCTIONS BEFORE COMPLETING FORM	
1. REPORT NUMBER	2. GOVT ACCESSION NO.	3. RECIPIENT'S CATALOG NUMBER	
Technical Report No. 263		AD-A100633	
4. TITLE (and Subtitle)	5. TYPE OF REPORT & PERIOD COVERED		
VERY LOW FREQUENCY TRANSMISSION LOSS IN SHALLOW WATER		9 Final Report	
7. AUTHOR(s)	6. PERFORMING ORG. REPORT NUMBER		
Raymond H. Ferris	15 N00014-81-C-0164		
9. PERFORMING ORGANIZATION NAME AND ADDRESS	10. PROGRAM ELEMENT, PROJECT, TASK AREA & WORK UNIT NUMBERS		
MAR, Incorporated 1335 Rockville Pike Rockville, MD 20852			
11. CONTROLLING OFFICE NAME AND ADDRESS	12. REPORT DATE		
Office of Naval Research, Code 464 Department of the Navy Arlington, VA 22217	11 May 81		
14. MONITORING AGENCY NAME & ADDRESS (if different from Controlling Office)	13. NUMBER OF PAGES		
12 155	50		
16. DISTRIBUTION STATEMENT (of this Report)	15. SECURITY CLASS. (of this report)		
UNLIMITED	UNCLASSIFIED		
17. DISTRIBUTION STATEMENT (of the abstract entered in Block 20, if different from Report)	15a. DECLASSIFICATION DOWNGRADING SCHEDULE		
18. SUPPLEMENTARY NOTES			
19. KEY WORDS (Continue on reverse side if necessary and identify by block number)			
Underwater Acoustics Transmission Loss	Shallow Water Very Low Frequency		
20. ABSTRACT (Continue on reverse side if necessary and identify by block number)	In this study, acoustic transmission loss is calculated at frequencies below cut-off for a shallow water duct. A highly idealized model, based on realistic estimates of the gross acoustic properties of the sea-bed, is used to calculate the energy distribution in range, frequency, and depth as functions of the major environmental parameters. Results show that values of loss, at frequencies below cut-off, are similar to those at the frequency of minimum loss above cut-off.		

DD FORM 1 JAN 73 1473

EDITION OF 1 NOV 65 IS OBSOLETE

S/N 0102-LF-014-6601

UNCLASSIFIED

SECURITY CLASSIFICATION OF THIS PAGE (When Data Entered)

390477

ABSTRACT

In this study, acoustic transmission loss is calculated at frequencies below cut-off for a shallow water duct. A highly idealized model, based on realistic estimates of the gross acoustic properties of the sea-bed, is used to calculate the energy distribution in range, frequency, and depth as functions of the major environmental parameters. Results show that values of loss, at frequencies below cut-off, are similar to those at the frequency of minimum loss above cut-off.

Accession For	
NTIS GRA&I	<input checked="" type="checkbox"/>
PTIC TAB	<input type="checkbox"/>
Unannounced	<input type="checkbox"/>
Justification	
Distribution/	
Availability Codes	
Avail And/or	
Dist	Special
A	

Table of Contents

	Page
Abstract	ii
List of Illustrations	iv
Executive Summary	1
Background	3
Approach	10
Results	13
Conclusions	33
References	38
Appendix A - Derivation of Transmission Loss Equations	39
Distribution List	47

List of Illustrations

	Page
1. General type of transmission loss range dependence.	5
2. Frequency dependence of transmission loss for a site off the coast of Florida.	7
3. Limiting ray paths for ducted propagation.	8
4. Attenuation coefficients of sediments.	11
5. Model used for calculating transmission loss at frequencies below cut-off.	12
6. Diagram showing annular strip on a sphere of unit radius about a point acoustic source.	12
7. Examples of ray paths.	14
8. Transmission loss dependence on sensor depth.	16
9. Dependence of transmission loss on water depth.	18
10. Dependence of transmission loss on the value of attenuation coefficient.	19
11. Attenuation of individual rays as a function of the product KfR.	20
12. Illustration of the differing range dependence of transmission loss for frequencies above and below cut-off.	22
13. Bounding values of transmission loss over the expected ranges of water depth and values of sediment attenuation coefficient.	23
14. Frequency dependence of transmission loss.	24
15. Departure from model predictions.	26
16. Transition from "no water-duct" to "water-duct" propagation.	27
17. Transmission loss data taken under environmental conditions departing strongly from those assumed in the model.	29
18. Comparison of model predictions with low-frequency transmission loss data.	32
19. Comparison of 8 Hz and 10Hz transmission loss data.	34
A-1 Diagram showing annular strip on a sphere of unit radius about a point acoustic source.	40
A-2 Examples of types of ray paths.	41
A-3 Diagram defining angles θ , θ_1 , θ_2 , and ϕ .	43

EXECUTIVE SUMMARY

Since 1948 when Pekeris¹ propounded the basic theory of acoustic propagation in a shallow water duct, there has been sporadic theoretical and operational interest in the special Sonar problems associated with shallow water. Until very recently, interest has been focused almost entirely on the frequency regime above the cut-off frequency of the duct (cut-off typically occurs between 5 to 25 Hz) where sound is effectively channeled between the water's surface and the sea-bed. Even with this channeling, the acoustic field is generally rapidly attenuated (relative to deep water propagation) because of losses incurred by the interaction of the acoustic field with the bottom. Below the cut-off frequency, sound cannot be trapped in the water but propagates both in the water and in the bottom sediments. Propagation characteristics in this low frequency regime have not been investigated sufficiently to allow an assessment of the potential performance of Sonar systems at frequencies below cut-off. This report documents the results of a study of the basic mechanisms affecting transmission loss at frequencies below cut-off in shallow water.

The environment is modeled as three fluid layers. The uppermost layer is isovelocity (1500 m/sec) water. The intermediate layer is an absorbing sediment having a positive sound speed gradient of 1 m/sec/m. The sound speed in the sediment matches that in the water at the interface, thus, no energy is trapped in the water duct. Below the sediment is a semi-infinite basement having a sound speed of 4,000 m/sec. An omnidirectional source is located in the water column. Using a special ray-theory model, the intensity of the acoustic field is calculated as functions of depth and horizontal range from the source, the results being expressed as transmission loss.

The results obtained with this idealized model disclose major trends and sensitivity to gross environmental parameters. Specific conclusions reached are listed below:

- With respect to depth, intensity is a maximum in the water. Below the water-sediment interface the intensity decreases rapidly with depth and the rate of decrease becomes greater with higher values of range, frequency, and the coefficient of attenuation in the sediments. In the statements which follow it is assumed that the sensor is located near the water-sediment interface.
- Transmission loss increases with range at a rate of approximately 4.5 dB per range doubled. At long ranges this characteristic differs significantly from that for frequencies above cut-off where the loss increase (expressed in dB) is nearly proportional to R rather than $\log R$.
- In general, as frequency is increased past cut-off, transmission loss can be expected to decrease as the energy becomes trapped in the water-duct.
- Transmission loss at frequencies below cut-off is comparable (not hugely greater or less) with that for ducted propagation at a few hundred Hz.
- Transmission loss increases with frequency at an approximate rate of 1.5 dB per frequency doubled.
- Transmission loss increases with water depth at a rate of approximately 1.5 dB per depth doubled, being about 5 dB higher at 500 m than at 50 m.
- Transmission loss increases with increasing coefficient of attenuation in the sediments. Over the expected range of values of the coefficient, 0.06 to 0.75 dB/m/kHz, the loss increases approximately 1.5 dB per doubling of the value of the coefficient.

- The thickness of the sediment layer has only a marginal effect on transmission loss for the range of thickness considered (50 to 1000m).
- A comparison with one data set which extended to frequencies below cut-off showed good agreement with transmission loss predicted by the ray-trace model.

Acoustic propagation in shallow water at frequencies below the cut-off of the duct does not appear to be inherently degraded relative to frequencies above cut-off. The relative performance of systems at very low frequencies is not apt to be defeated by high transmission loss. On the other hand, very low frequencies do not offer any marked advantage here relative to frequencies of a few hundred Hz. An assessment of relative system performance must hinge on a combined evaluation of all major factors in passive system performance including transmission loss, ambient and self noise, target radiation spectra, and limitations on temporal and spatial signal processing.

BACKGROUND

Passive acoustic detection of submarines in shallow water conventionally relies on sensing that portion of target radiated noise which is propagated in the duct between the reflective boundaries of the water column, i.e., the air-water and the water-sediment interfaces. Detection via this mode is limited to frequencies well above the cut-off frequency of the duct since, below cut-off, the acoustic field cannot be trapped in the water column. The frequency of cut-off depends primarily on the sound-speed ratio at the water-sediment interface and on the water depth. Typically it is in the range 5-25 Hz.

Numerous measurements of shallow water transmission loss have been made and reported - mainly within the past decade. With only a few exceptions the measurements were confined to frequencies above about 100

Hz. Contributing reasons for the sparsity of low-frequency data are (1) difficulty of obtaining high-power, calibrated, low-frequency sources; (2) high self-noise in sensor systems at low frequencies; and (3) formerly, a lack of interest in low frequency data.

Studies of available data together with the use of deterministic, wave-theory models, has led to a good understanding of the general characteristics of propagation for frequencies well above the cut-off frequency. Quantitative predictions for specific sites is hampered principally by lack of knowledge of environmental parameters.

In ducted transmission at frequencies well above cut-off, the range dependence of transmission loss can, in a general way, be characterized by three terms, one for the initial excitation, one for the geometric spreading, and one for attenuation. Numerous investigators have concluded that the simple expression

$$TL = A + 10 \log R + aR; \quad (1)$$

where TL is the transmission loss expressed in dB, A is a constant, R is the range in km, and a is an attenuation coefficient; provides a reasonable (although not precise) representation of the general range dependence. Figure 1 shows a comparison of this function with that for spherical spreading. The value of a used is 0.5, a value representing moderate to high loss conditions at 200 Hz. As is typically the case, the loss is less than spherical spreading for a few tens of kilometers and becomes precipitously higher at longer ranges. It will be shown later that this characterization does not hold at frequencies in the vicinity of cut-off and lower.

With regard to frequency dependence of transmission loss, there are several characteristic features for the frequency regime above about 100 Hz. First, there is always a frequency of minimum loss, which usually occurs below 500 Hz. It has been observed that the frequency at which the minimum occurs increases with increasing range. It was shown in reference (2) that, for frequencies above that of minimum loss, there is empirical

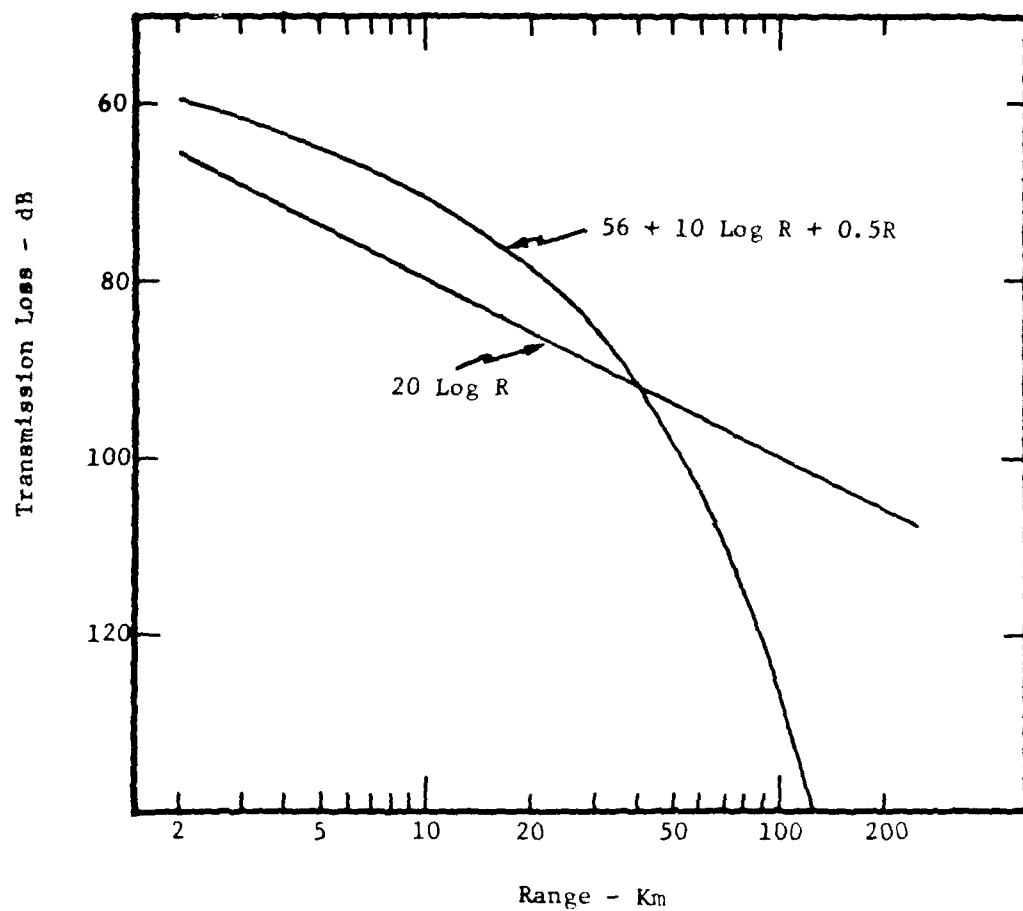


Figure 1. General type of transmission loss range dependence
in a shallow water duct at frequencies above cut-off
compared with spherical spreading.

evidence suggesting that loss increases exponentially with frequency and the rate increases both with range and with the loss condition, i.e., the higher the transmission loss at any given frequency and range, the higher the rate of increase with frequency. Further, it was shown that for frequencies above that of minimum loss the frequency dependence was consistent in the sense that if the loss is known at any particular frequency and range, values of loss at other frequencies and ranges can be estimated from a simple expression.

Figure 2 illustrates the frequency dependence of transmission loss observed in a data set taken in water depth of 200 feet, off the coast of Florida in October (derived from data given in Reference 9, page 167). This shows the loss minima which occur at increasing frequencies with increasing range. Above the frequency of minimum loss the loss increases at increasing rates as range is increased. Below the minima the loss increases as cut-off frequency is approached.

At frequencies above a few hundred Hz, the acoustic field at all except very short ranges results from energy propagated in the discrete normal modes³ of the duct. The source energy which contributes to the field is that portion emitted at vertical angles between $\pm \theta_c$ where θ_c is the critical grazing angle at the water-sediment interface (see Figure 3). Energy emitted at larger angles can reenter the water via refracted paths (dashed line) but it is highly attenuated by absorption in the sediment and makes no significant contribution to the field. For example, at 1 kHz, attenuation is at the rate of 60 to 750 dB per km using the range of values of attenuation coefficient reported by Hamilton⁴. The attenuation coefficients are thought to be linearly dependent on frequency and so, as frequency is reduced, the refracted paths begin to make significant contributions. At frequencies below cut-off the discrete normal modes no longer exist and all propagation paths are, at least partially, in the sediments.

The purpose of this study is to calculate the transmission loss to be expected at frequencies below cut-off. A highly idealized model based on realistic estimates of the gross acoustic properties of the sea-bed is used to calculate the energy distribution in depth, range, and frequency.

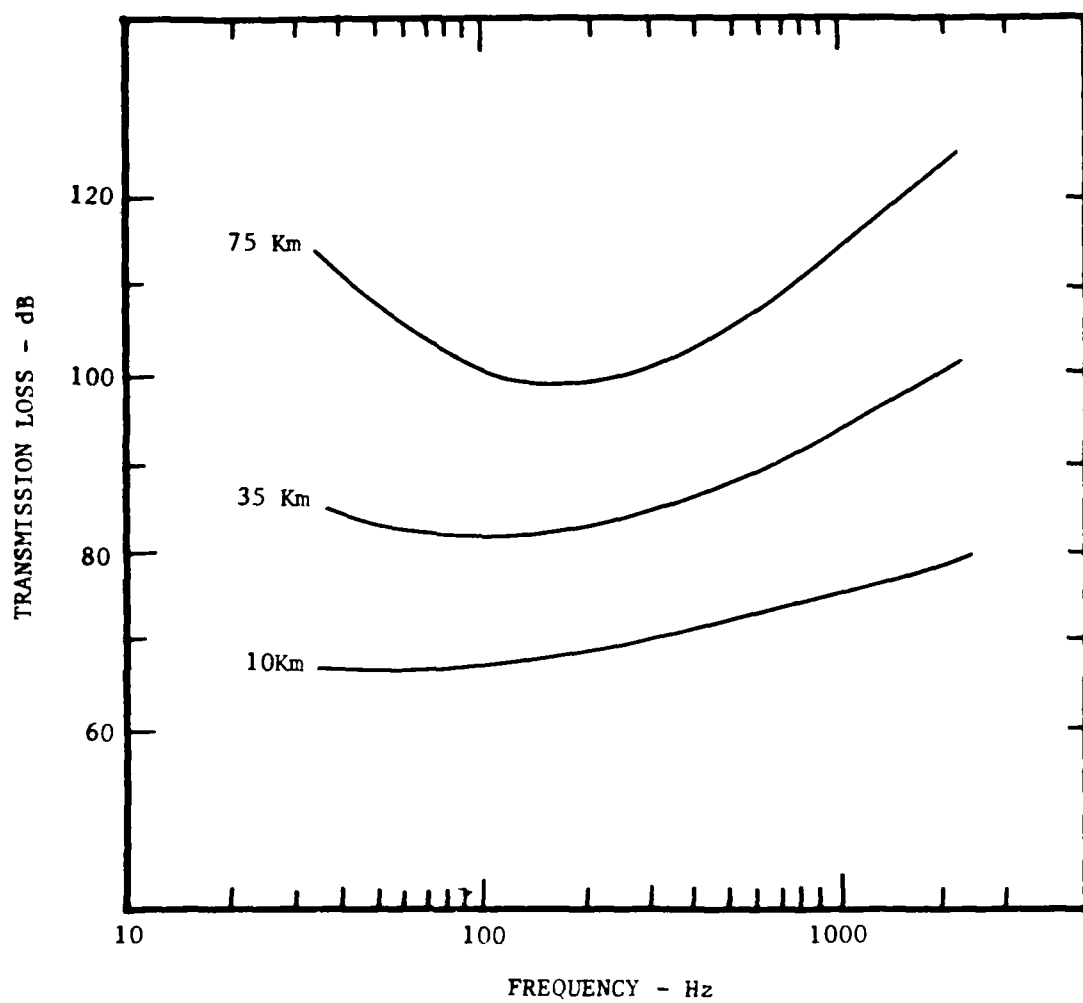


Figure 2. Frequency dependence of transmission loss for a site off the coast of Florida (Urick).

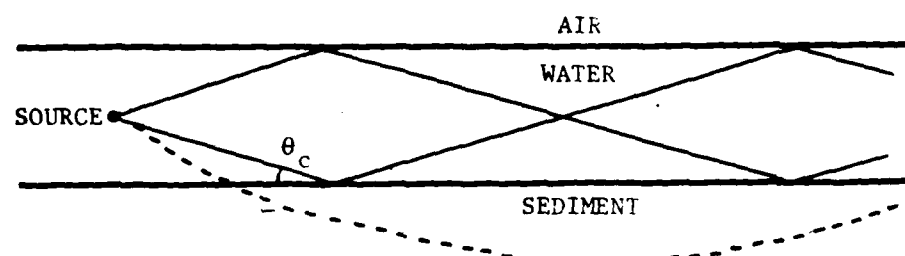


Figure 3. Limiting ray paths for ducted propagation in shallow water (solid lines). Steeper rays enter the bottom sediments (dashed line).

In reference (5) Hamilton discusses geoacoustic models of the sea floor. With regard to shallow water he states, "A common stratigraphy in continental shelves is a top layer of soft mud, or clay-silts, overlying harder silts and sands. This is common because during lowered sea levels of the Pleistocene sand was deposited over wide areas of the shelf, and then covered with silt-clays as sea levels rose." Houtz and Ewing⁶ reported the results of seismic profiling along the western North Atlantic margin from about 21° to 42° North Latitude. Of 54 stations reported, 16 were on the upper part of the continental rise with water-depths ranging from 80 to 2860 meters. The sediment thickness (consolidated plus unconsolidated) for these shallower stations ranged from about 1800 to 5000 m with an average thickness of 3400 m. The uppermost, unconsolidated part of the sediments ranged in thickness from about 600 m to 2400 m with an average of 1500 m. The sound speeds in the basement, underlying the sediments, ranged from about 4000 to 5000 m/sec. The sound speed in the sediment layer normally increases with depth. Hamilton⁷ reported the results of measurements from 20 areas. The average values of gradient ranged from 1.3 m/sec/m in the upper part of the sediments to 0.6 m/sec/m at a depth of 1000 m. Hanna⁸ quotes an expression for the specific variation of sound speed, C, with depth in the sediments (as derived by Houtz and Ewing) as:

$$C = C_1 [1 + 2 (g/c) Y]^{1/2},$$

where c and g are the sound speed and its gradient at the interface, and Y is depth below the interface. In most shallow water areas the sound speed in the sediment at the water-sediment interface is a few percent higher than the sound speed in the water. At frequencies above cut-off this is very important since it enables ducted propagation in the water column. At frequencies below cut-off this small perturbation in the sound speed profile has little effect and, in the low-frequency model we use, it is neglected.

The sediments are absorbing and, although it is difficult to determine experimentally, the absorption is commonly considered to increase linearly with frequency. Hamilton⁵ states that, "There is no single data set covering more than two orders of magnitude in frequency, and data is scarce below 1 kHz. These data are enough to show that dependence of attenuation on frequency is more nearly f^1 than $f^{1/2}$ or f^2 (but not enough to verify an exact dependence) for the following: silt-clays or muds from a few Hz to at least 1 MHz, and from 1 kHz to at least 1 MHz for sands, and from 150 Hz to 1 MHz for mixed types." Hamilton⁴ reports a regression fit to various data for the attenuation coefficient, k , as a function of grain size of the sediments as shown in Figure 4. Values of k range from 0.06 to 0.75 dB/m/kHz.

APPROACH

As shown in Figure 5, the environment is modeled as three fluid layers. The uppermost is water having a constant sound-speed of 1500 m/sec and a thickness of H_1 . The water overlies a sediment layer of thickness H_2 having a sound-speed at the top of 1500 m/sec and a positive sound-speed gradient of 1 m/sec/m. Beneath the sediment is a semi-infinite, high-speed layer having a constant sound-speed of 4000 m/sec. An omnidirectional acoustic source of source level I_0 is located in the water. For this model, the results are independent of source depth.

The distribution of the acoustic field is obtained by tracing the power emitted in narrow segments in vertical angle from the source as shown in Figure 6. Segment widths of either 2° or 0.2° , depending on desired resolution, have been used in computations reported here. Analysis is performed in three dimensions. However, since azimuthal symmetry is assumed, results are given in terms of range and depth only. Rays, traced from the center angle of each segment, are assumed to carry the total segment power. The total power of the source ($4\pi I_0$) is assumed to be conserved except for that lost through two mechanisms. In the first, those rays which reach the fast layer at grazing angles greater than the critical

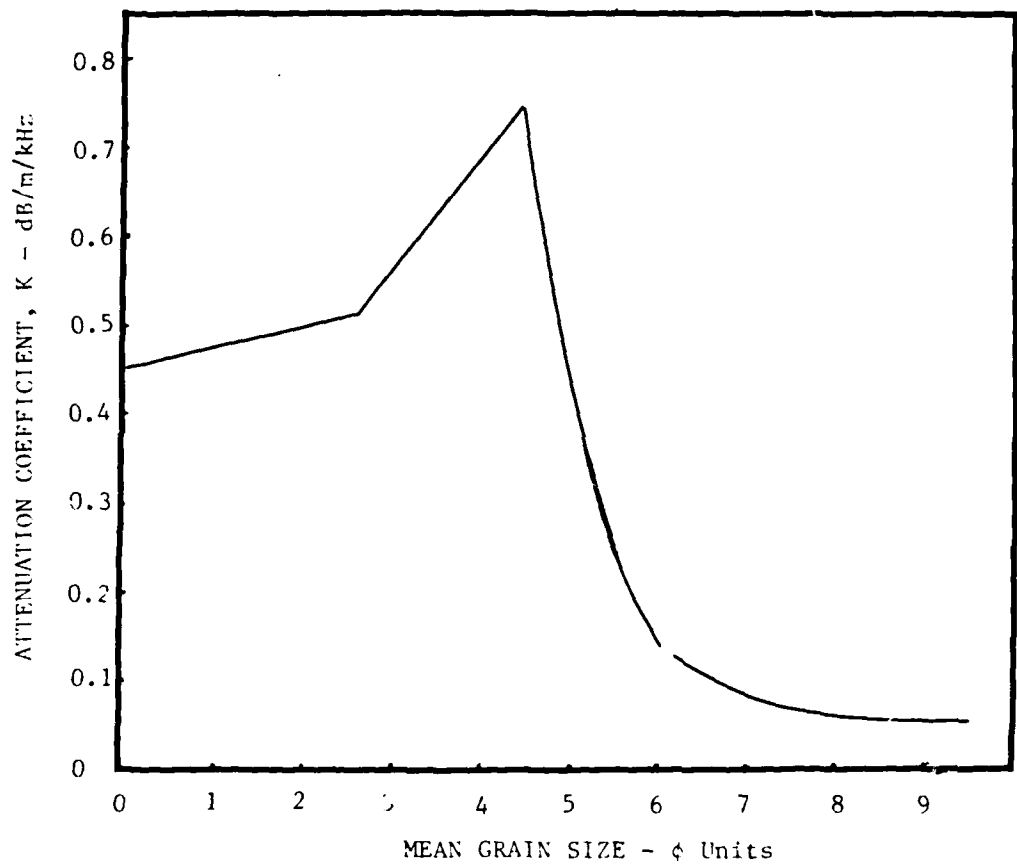


Figure 4. Attenuation coefficients of sediments

Regression fit (from Hamilton) to data on attenuation coefficients of sediments.

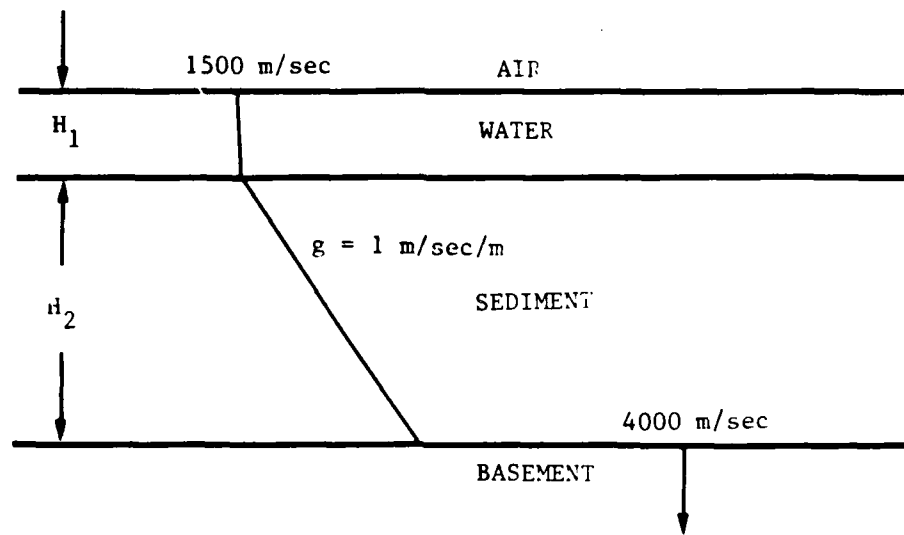


Figure 5. Model used for calculating transmission loss at frequencies below cut-off

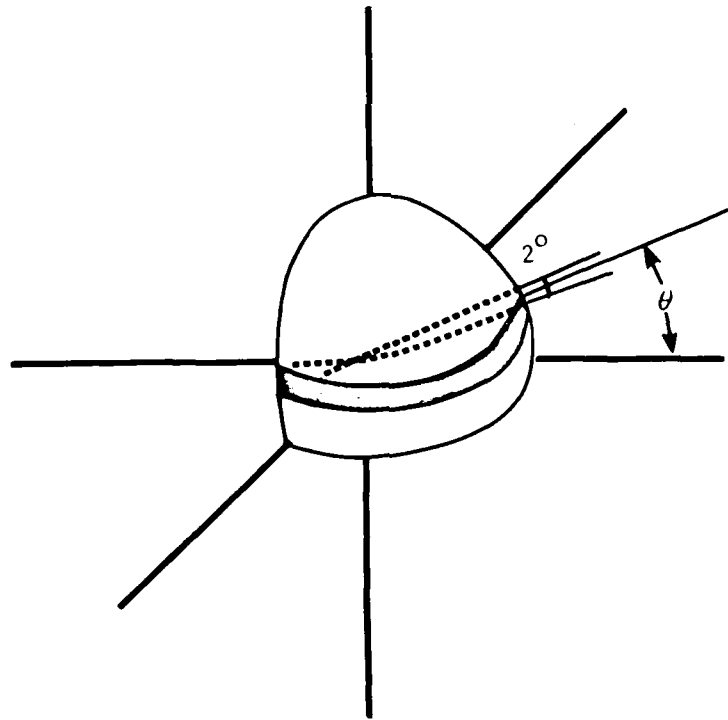


Figure 6. Diagram showing annular strip on a sphere of unit radius about a point acoustic source at the origin. The power crossing the the annular strip is assigned to the ray which bisects the strip at vertical angle θ .

are assumed to penetrate the layer and their power is lost. It is shown in Appendix A that, because of the assumed model geometry, rays leaving the source at vertical angles greater than 68° penetrate the fast layer and this is independent of the depth of sediments. The second loss mechanism considered is that of absorption in the sediment. It is assumed that, while propagating in the sediment layer, each ray is attenuated at the rate of Kf where K is the attenuation coefficient in $\text{dB}/\text{m}/\text{kHz}$ and f is the frequency in kHz. In computational examples given, values of K of 0.06, 0.40, and 0.75 are used. These correspond to minimum, mean, and maximum values of a regression fit to data reported by Hamilton⁴.

In order to obtain the distribution of the field with depth, the sediment is divided into an arbitrary number of layers. The contributions of intensity from each source segment are then summed within each sediment layer and in the water column as a function of range. To avoid small-scale fluctuations with range, the contribution of each ray at any given range is taken as being proportional to the probability of the ray being within that depth interval rather than its presence or absence at that particular range. Also, absorption is calculated as being proportional to the ratio of path length in the sediments to horizontal advance in range averaged over range. The results are given as transmission loss defined as $10 \log \frac{I_0}{I}$ where the intensity, I , is defined as power crossing a unit area normal to the horizontal range vector. Derivations of the equations used in calculating transmission loss are given in Appendix A.

RESULTS

The model described is intended for the calculation of transmission loss characteristics when the propagation field is not trapped in a water-duct. The term water-duct, as used here, refers to cases where sound is confined within the water column by some combination of reflection and/or refraction as shown in Figures 7(a),(b) and (c). The ray paths shown apply only at frequencies above cut-off. The model used here

SOUND - SPEED
PROFILES

RAY - PATHS

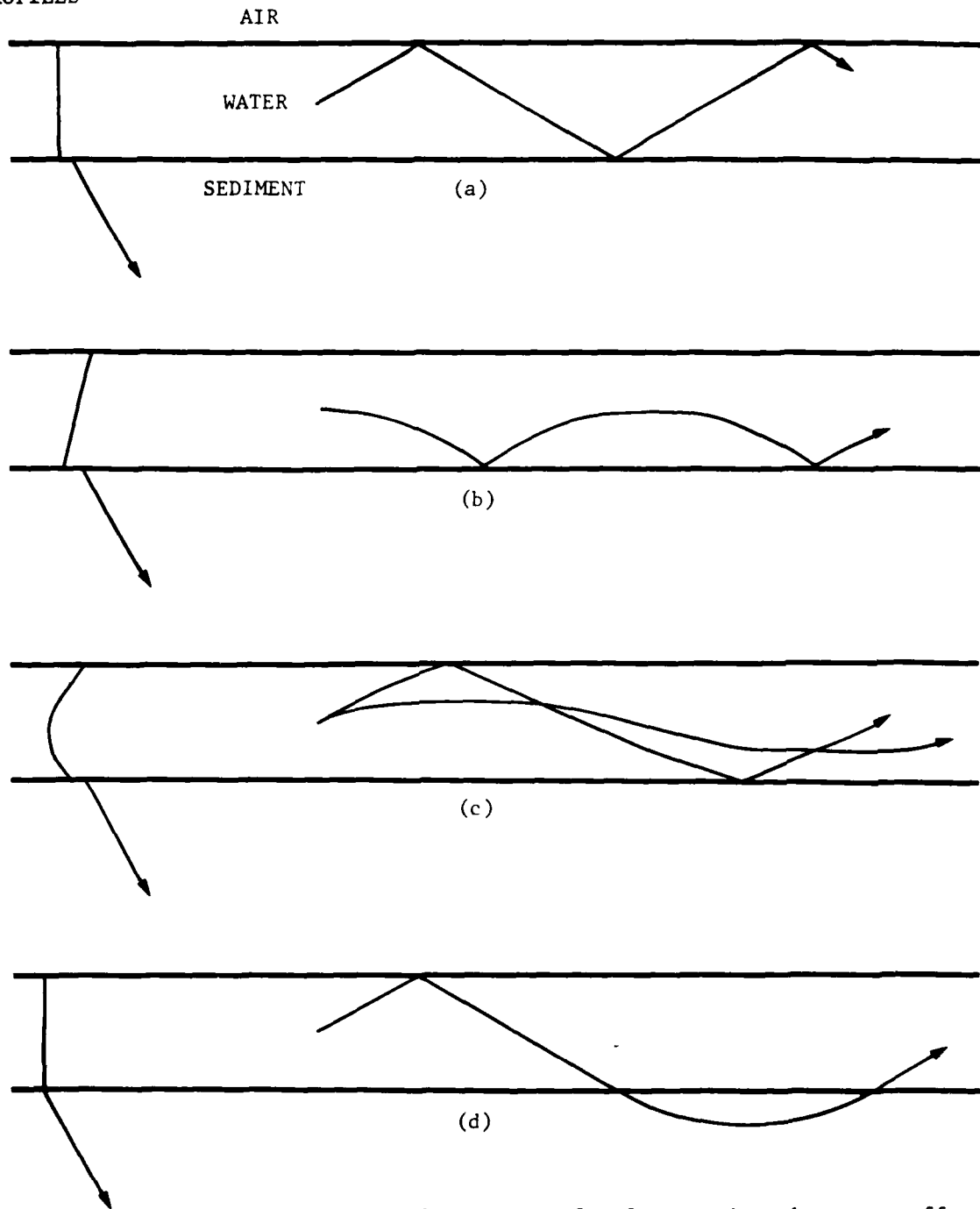


Figure 7. Examples of ray paths for frequencies above cut-off (a through c) and for frequencies below cut-off (d).

provides no water-duct and all propagation paths include propagation in the sediments as shown in Figure 7(d). Results of calculations will now be shown providing estimates of loss characteristics at frequencies below cut-off and giving some insight concerning expected behavior in the transition region.

First, examples of the dependence of transmission loss on sensor depth, sediment thickness, water depth, attenuation coefficient, range, and frequency will be shown. This is followed by a consideration of the transition from the condition of no water-duct to propagation in a water-duct as frequency is increased past cut-off. An example of comparison with measured data is shown. Variables considered include the horizontal range from the source, R ; the frequency, f ; the water depth, H_1 ; the sediment thickness, H_2 ; the attenuation coefficient in the sediment, k ; and the sensor depth.

In order to illustrate the distribution of energy with depth in the water and in the sediments, the transmission loss was calculated as a function of sensor depth. A water depth of 100 m and an attenuation coefficient in the sediments of 0.4 dB/m/kHz were assumed. Calculations were made for each of three values of sediment thickness, 50, 200 and 1000 m; three frequencies, 5, 10, and 20 Hz; and two ranges, 10, and 20 km. The results are shown in Figure 8. On the left side, loss vs depth at 10 km is given for the three values of sediment thickness, 1000m (top), 200 m (center), and 50m (bottom). In each case the loss is plotted for each of the three frequencies. Results are given in the same format on the right side for a range of 20 km. Several features are apparent. The loss increases rapidly with depth below the water-sediment interface, and the rate of increase increases with range and frequency. The loss to a point in the water column is affected only very slightly by thickness of the sediment layer for the range of thicknesses considered here. Loss is a much stranger function of frequency in the sediments than in the water column.

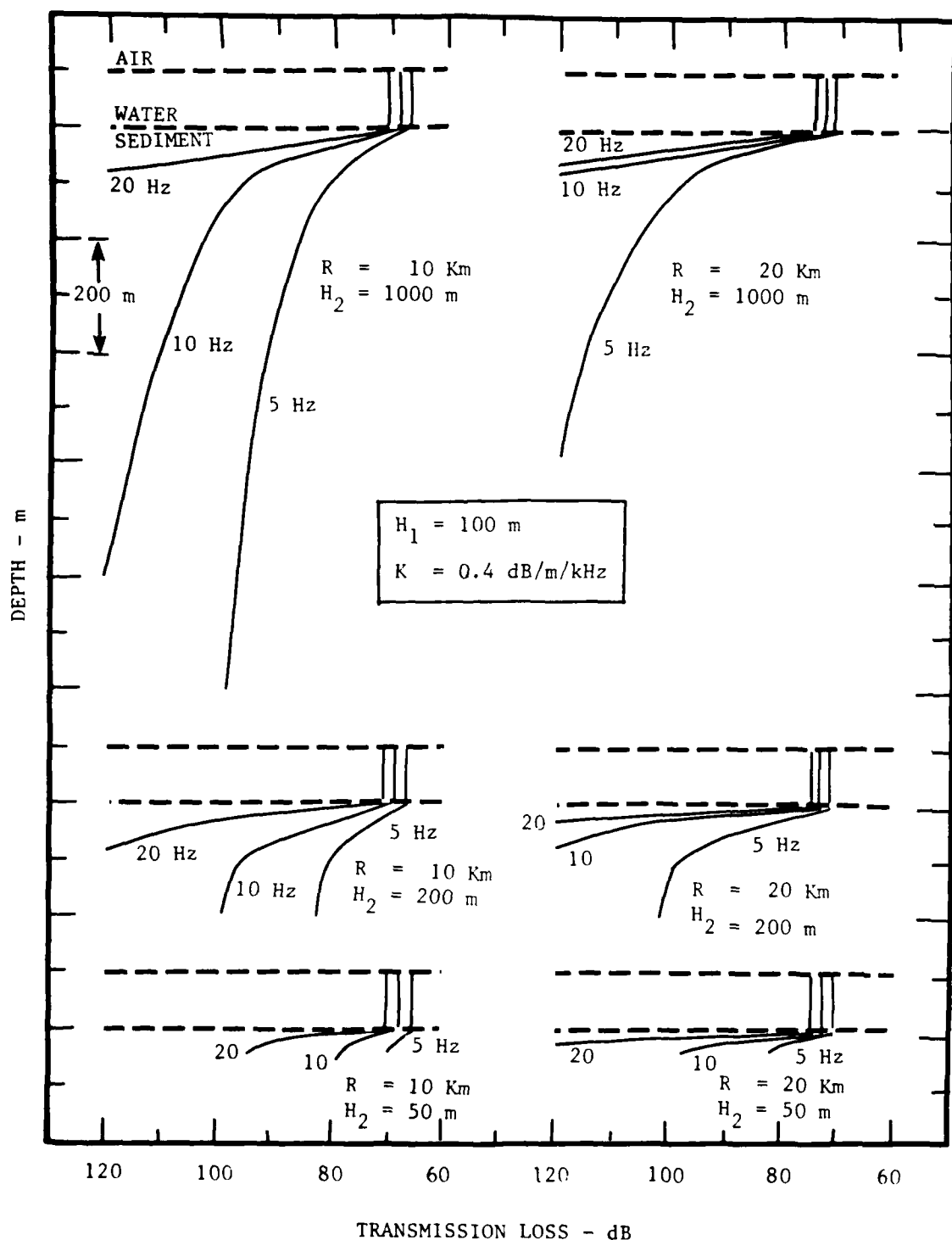


Figure 8. Transmission loss dependence on sensor depth in the water and sediments at a range of 10 km (left) and 20 km (right). Losses are shown for each of three frequencies and for sediment thicknesses of 1000 m (top), 200 m (middle), and 50 m (bottom).

It should be noted that, although the intensity is independent of sensor depth in the water, the excess pressure is not since it must be zero at the surface. A pressure sensor should be positioned at least one quarter of a wavelength from the water's surface.

An example of the dependence of transmission loss on water depth is shown in Figure 9. The tenfold increase in water depth (50 to 500m) results in a 10 dB increase in spreading loss. This is counteracted in part by the decreased ratio of path-length in the sediment to range-advance. The combined result shown in Figure 9 - approximately 5 dB increase in loss for a water-depth increase from 50 to 500 m - indicates only a moderate sensitivity to water depth.

Figure 10 shows results of calculation of transmission loss as functions of K. In the interval of K from 0.06 to 0.75 the transmission loss increases less than 6 dB. This might seem to be a surprisingly moderate dependence on K. It stems from the special manner in which transmission loss is governed by change in the values of K, f, and R. As values of these variables are increased, the deeper going rays are rapidly attenuated and are stripped off, whereas the shallower rays are only slightly affected. Transmission loss is controlled, therefore, by the number of low-loss rays contributing to the field. Even though an increase in K, f, or R, can cause an enormous increase in the attenuation of steeper (deep-going) rays, if the result, for example, is to effectively remove one half of the rays, the loss increases by only about 3 dB. Figure 11 illustrates the degree to which rays, which leave the source at vertical angles ranging from 0.25° to 64° , are attenuated by absorption in the sediments (exclusive of spreading loss). The rapid increase of attenuation with the steepness of the ray angle is apparent. It can also be seen, however, that for any value of KfR less than 1000, there is always a range of angles over which the attenuation is negligible.

The fact that transmission loss is governed by the stripping off of rays results in a markedly different loss versus range characteristic than in the case of propagation in a water duct. It was seen in Figure 1 that, at long ranges, loss in a water-duct is dominated by the absorption term,

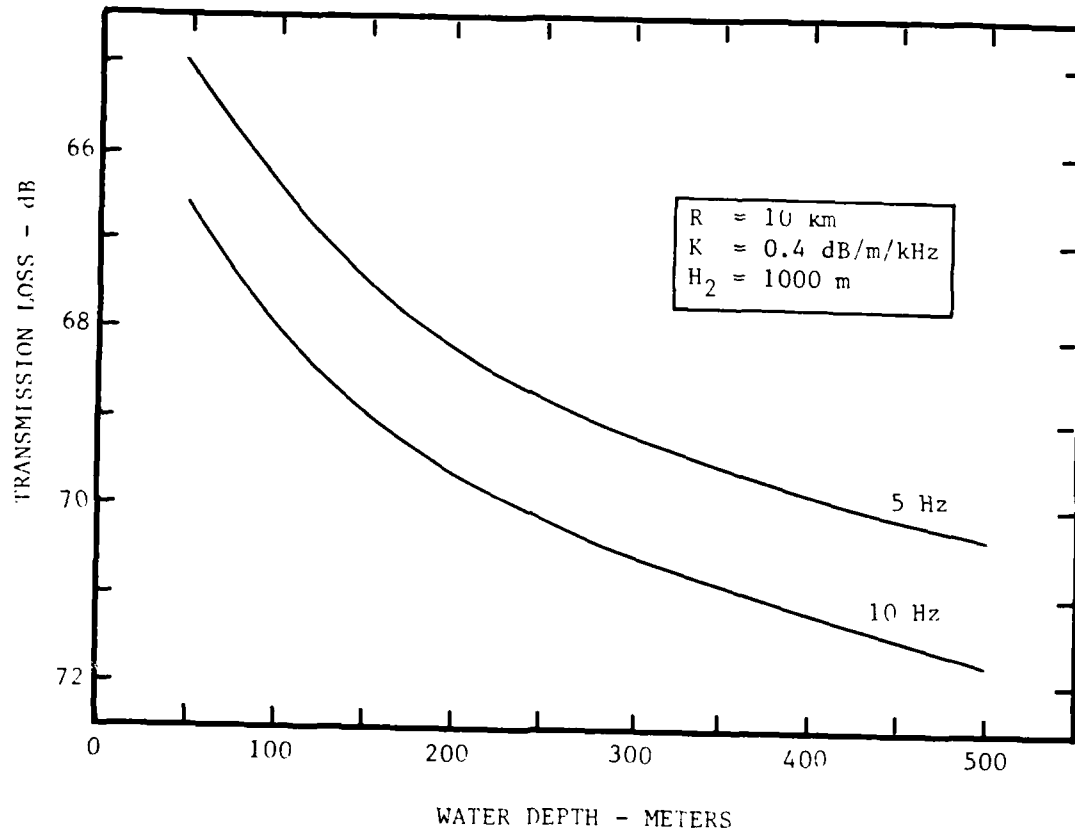


Figure 9. Dependence of transmission loss on water depth

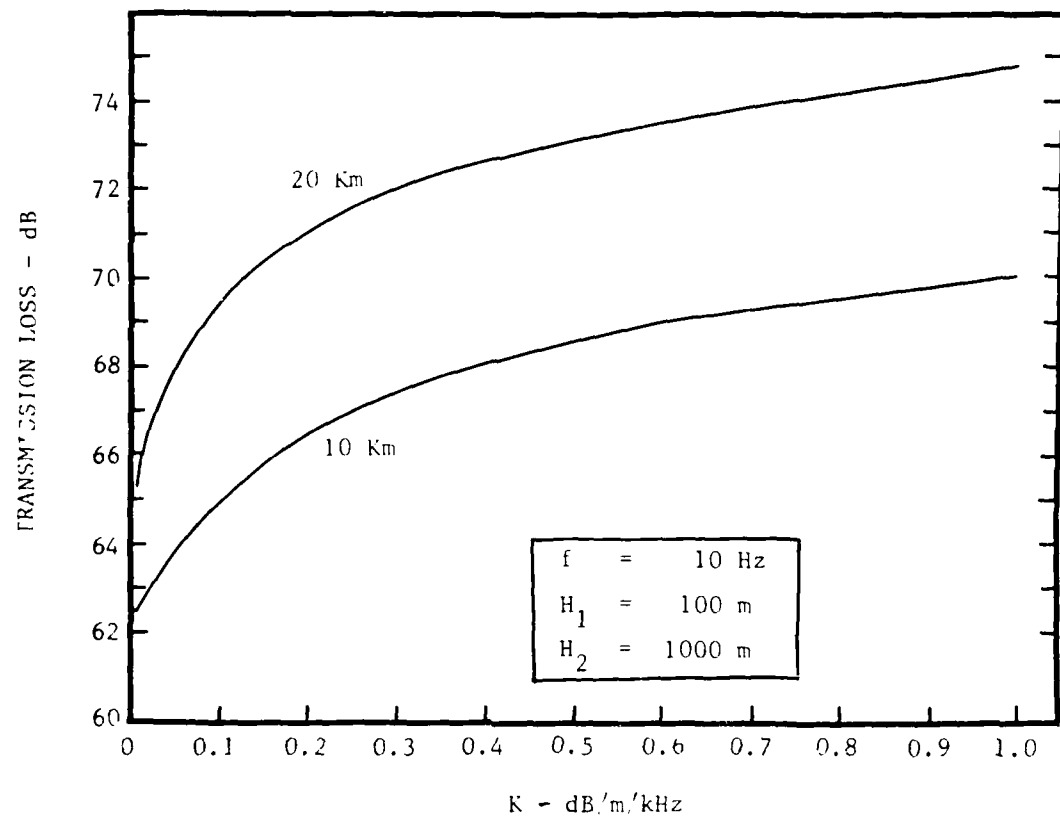


Figure 10. Dependence of transmission loss on the value of attenuation coefficient in the sediments, K.

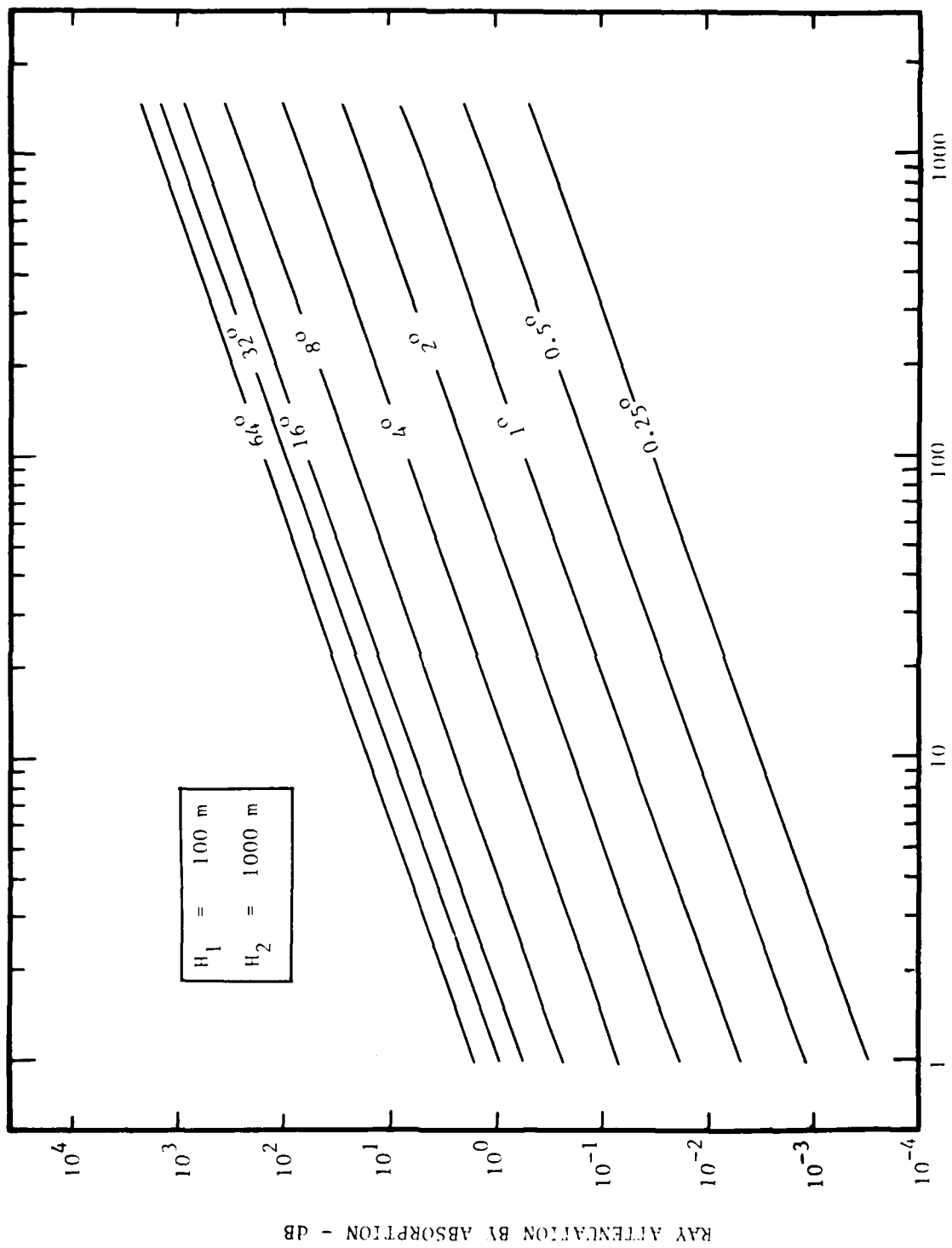


Figure 11. Attenuation of individual rays as a function of the product KfR where K is the attenuation coefficient of the sediments in $\text{dB}/\text{m}/\text{kHz}$, f is the frequency in kHz , and R is the range in meters. The attenuation is that resulting from absorption only (spreading loss not included).

a R. In Figure 12, Calculated loss vs range for the no water-duct case at 10 Hz is compared with a typical curve for 200 Hz in a water-duct having moderately high loss. The no water-duct curve is nearly a straight line when, as here, a logarithmic range scale is used. The slope is nearly proportional to $\log R$ for the no-duct case rather than to R as in the ducted case. Although the losses are comparable at short ranges, the no-duct case does not suffer the precipitously high loss at long ranges.

The combined effect of water depth and attenuation coefficient is shown in Figure 13. Water depths of interest for anti-submarine warfare on the continental shelves can probably be considered to be in the range of 50 to 500 meters. We have seen that attenuation coefficients for sediments can be expected to range from 0.06 to 0.75 dB/m/kHz. Those limiting values are used in obtaining the bounding curves of transmission loss vs range at a frequency of 10 Hz shown in Figure 13.

The dependence of loss on frequency is illustrated in Figure 14 for each of three ranges and each of two values of attenuation coefficient. Again, as with the dependence on K , the rate of loss increase with frequency, is low. At the higher frequencies and long ranges, the energy is carried by a narrow bundle of rays which have only a small fraction of their path lengths in the sediment.

In most, but not all, shallow water areas, the ratio of the sound speed in the sea-bed to the sound speed in the water at the interface is greater than unity. In sediments consisting of certain clays the ratio can be less than unity but this is probably a rare occurrence. In most cases, then, a water-duct exists at sufficiently high frequencies. As the frequency is increased from below to above cut-off, the propagation mode will transition from no water-duct to that of a water-duct. At and above cut-off the model used here is not valid. In transitioning to water-duct propagation one would expect the transmission loss to decrease although there are, perhaps, certain cases (such as with extremely rough boundaries) where this would not occur. Assuming that the loss decreases, the change in slope of the loss vs frequency curve should occur in the vicinity of the cut-off frequency.

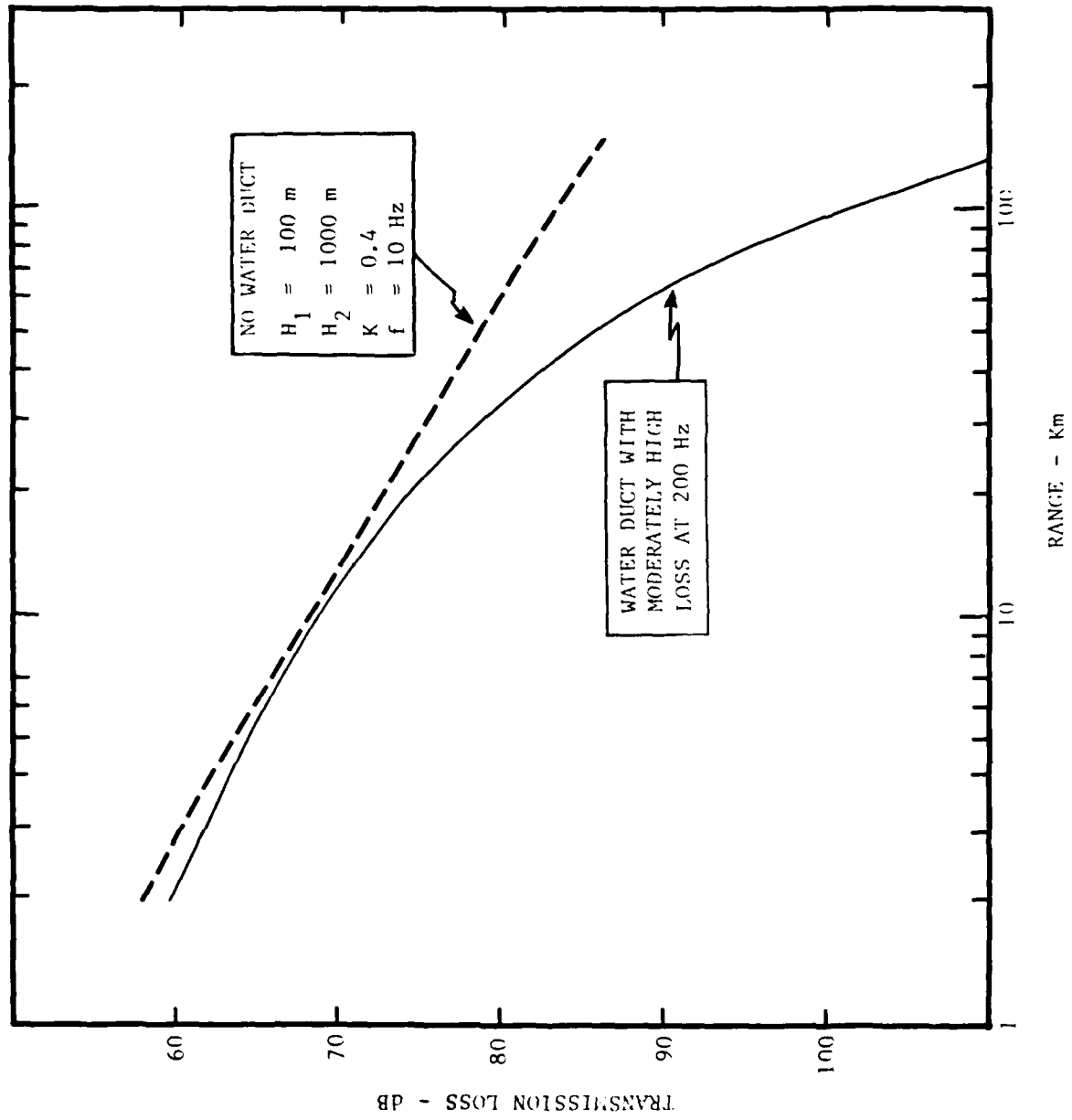


Figure 12. Illustration of the differing range dependence of transmission loss for frequencies above and below cut-off

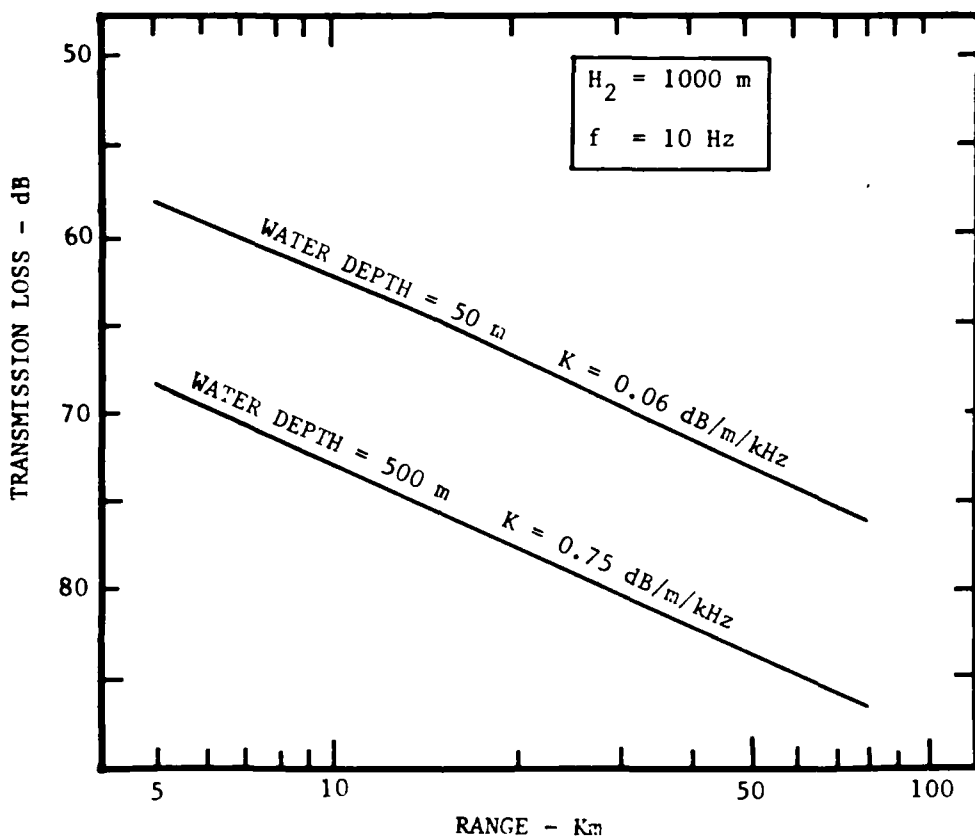


Figure 13. Bounding values of transmission loss over the expected ranges of water depth and values of sediment attenuation coefficient.

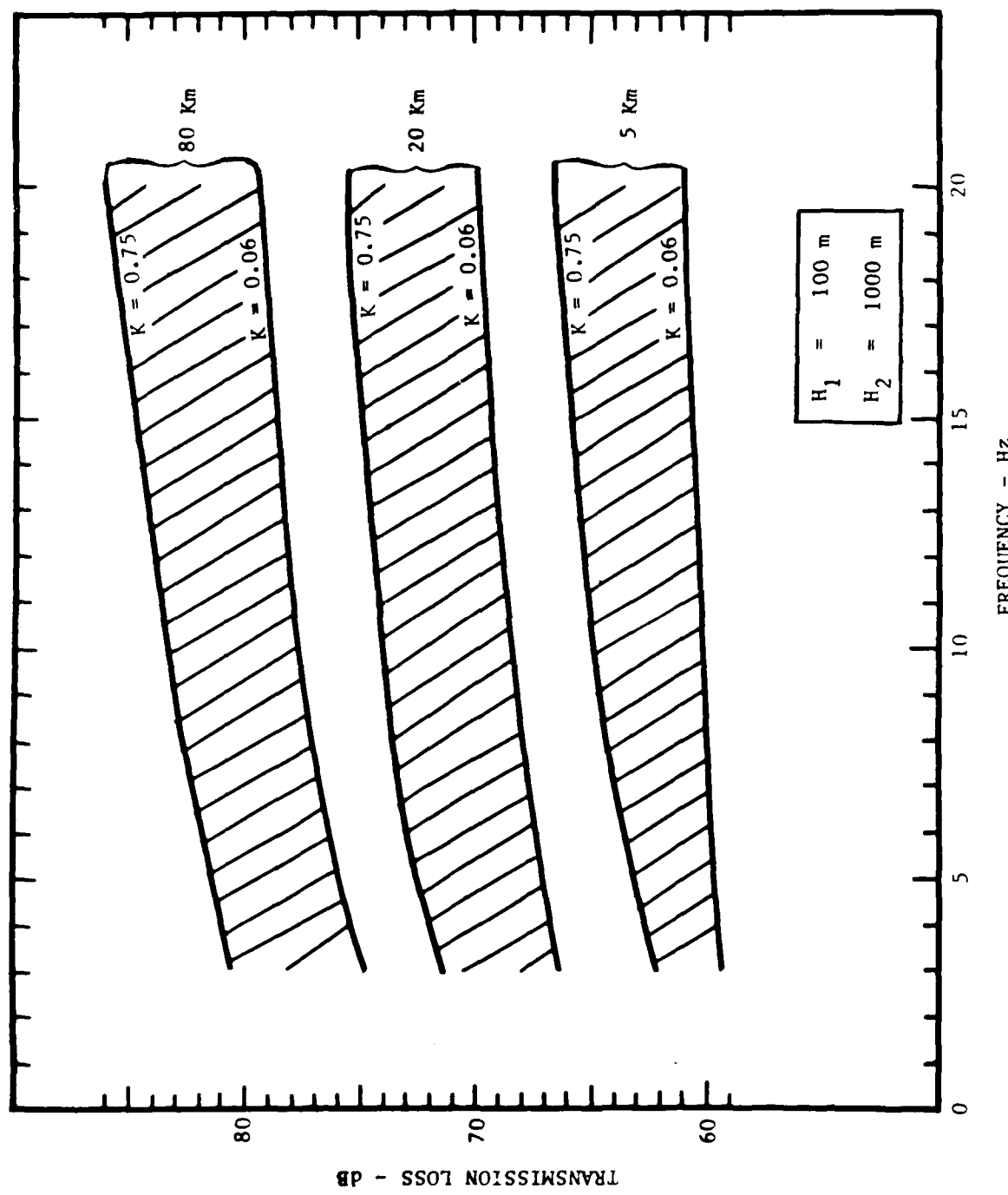


Figure 14. Frequency dependence of transmission loss

In Figure 15, calculated loss vs frequency for no water-duct propagation is plotted together with break-off points where the model is no longer valid at cut-off frequencies for various values of C_2/C_1 , where C_2 is sound-speed in the sediment and C_1 is sound speed in the water, both at the interface. Cut-off frequency, f_o , is calculated from the equation:

$$f_o = \frac{C_1}{4H_1} \sqrt{\frac{1}{1 - (C_1/C_2)^2}}$$

The points of intersection of the dashed lines with the solid line occur at the cut-off frequency corresponding to the indicated values of the ratio C_2/C_1 . At those points, the dashed lines indicate the expected direction of deviation of loss from the values calculated by the model. The solid line and its extension (dotted line) represent the calculated loss for the condition of no water-duct. The expected loss versus frequency function, therefore, would follow the solid line starting at 3 Hz up to the cut-off frequency. Although not shown in Figure 15, it is expected that, as the frequency continues to increase, the loss would pass through a minimum and then continually increase.

Ross and Adlington, in an informal communication¹⁰, reported results of transmission loss measurements in an area on the Canadian continental shelf north of Grand Banks. The sound speed profile displayed a sound speed minimum in the water column resulting in low loss conditions. Measured loss vs frequency at a range of 100 km is plotted in Figure 16 (lower solid line). The losses at 100 km were obtained by averaging (using linear power scale) the reported transmission loss over the range interval from 90 to 110 km. The upper solid line represents our calculation with the no water-duct model using the mean water depth of the area and an assumed value of 0.4 dB/m/kHz for the attenuation coefficient of the sediments. The dashed line is the author's conjecture of how the data, if carried to lower frequencies, might make the transition from duct to no-duct losses. The sound speed ratio at the bottom is not known and, therefore the cut-off frequency cannot be calculated accurately. The value shown (6 Hz) is for an assumed ratio of $C_2/C_1 = 1.03$.

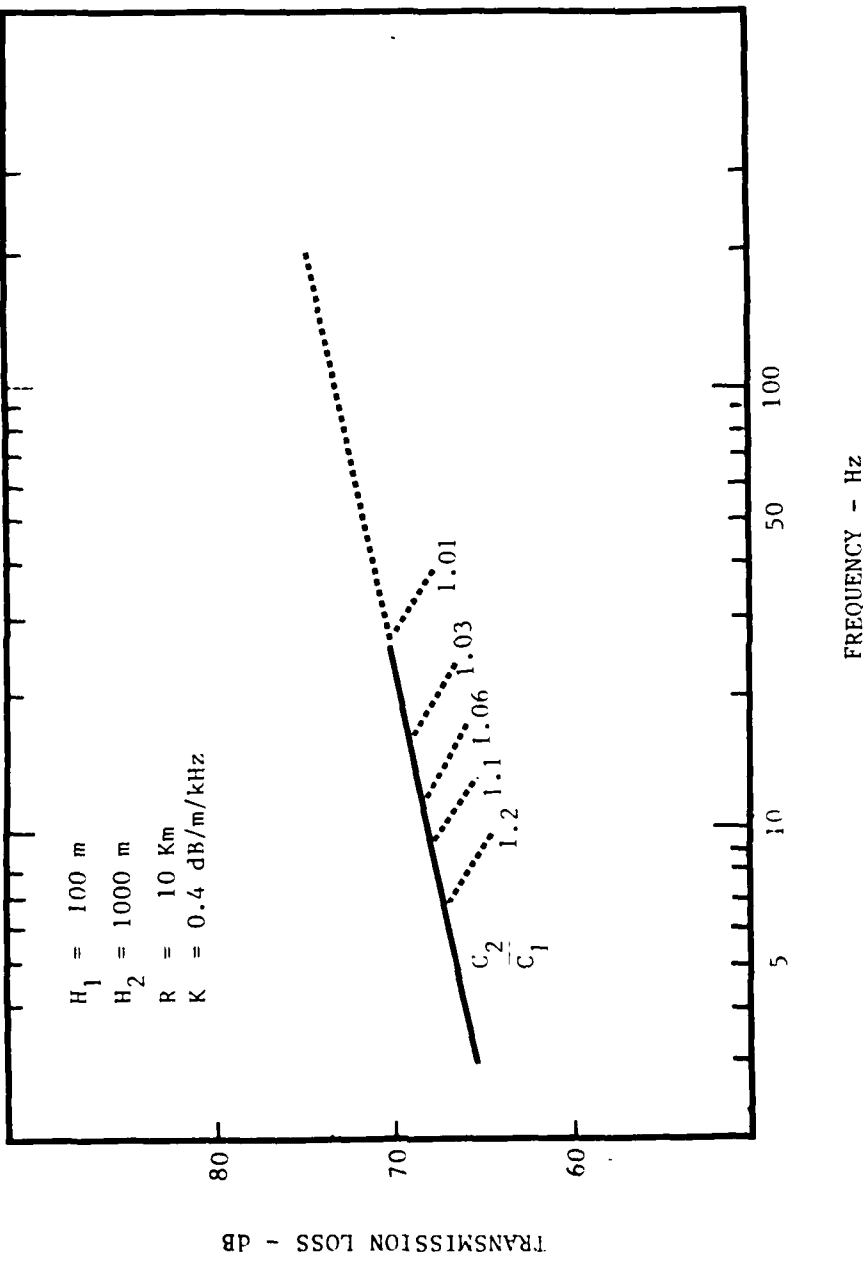


Figure 15. Departure from model predictions. The solid line and its dotted extension represent model predictions. The dashed lines show expected departure from model predictions as frequency increases past cut-off. Several values of cut-off frequency (intersection of solid and dashed lines) are shown depending on the ratio of the sound speed in the bottom (C_2) with the sound speed in the water (C_1) at the interface.

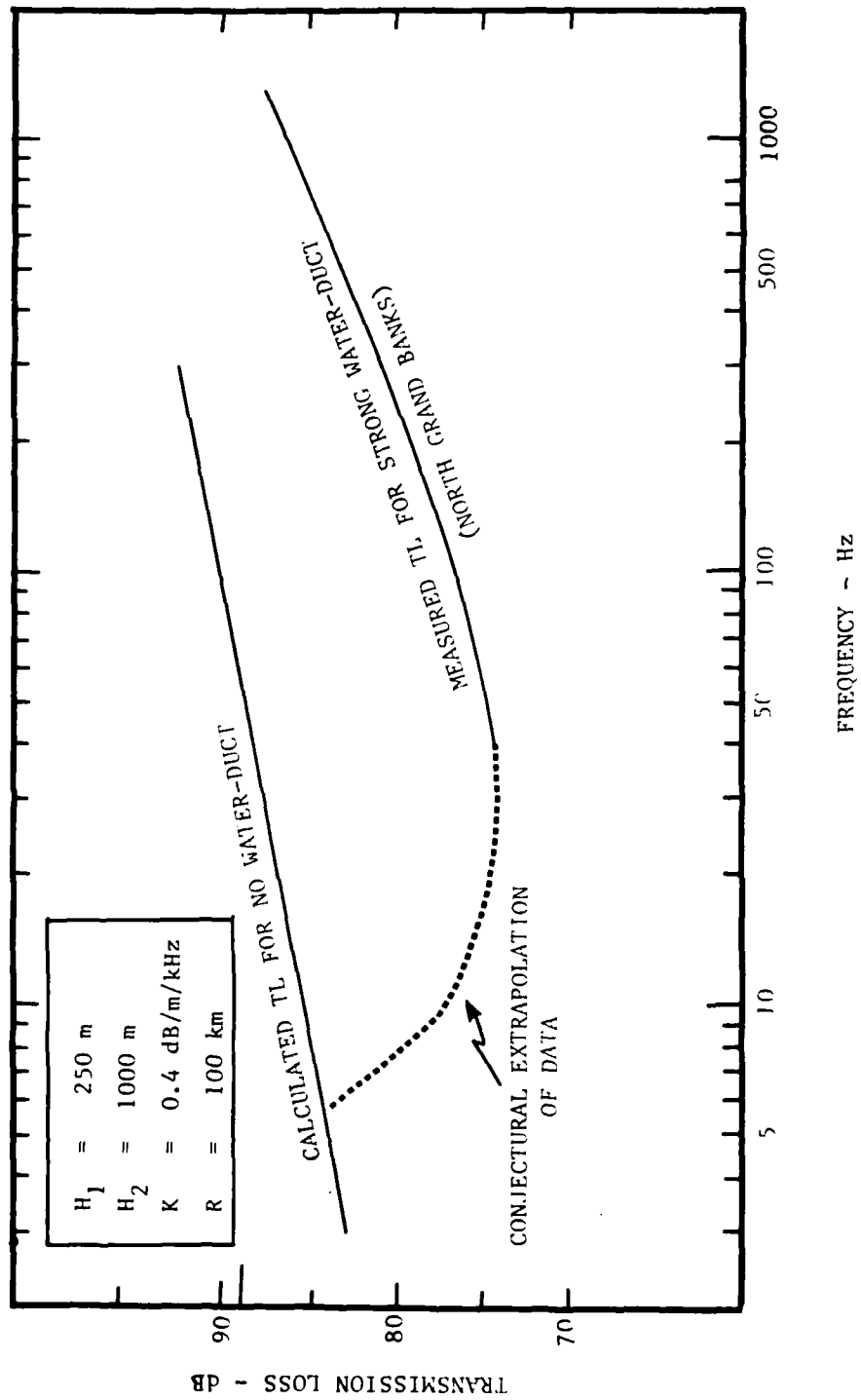


Figure 16. Transition from "no water-duct" to "water-duct" propagation. The upper solid line shows predicted loss for the model which does not allow a water-duct. The lower solid line is measured data (Ross and Adlington) for a condition of a strong water-duct. The dashed line represents a possible transition path as frequency is lowered toward cut-off.

Data from another area, South Grand Banks also were reported by Ross and Adlington¹⁰. In this case there was a strong, downward refracting sound speed profile in the water having an average gradient of about - 0.7 m/sec/m. The topography of the sea-bed was undulating with water depth varying between approximately 81 and 106 m. The reported transmission loss was very high as would be expected with such a strong negative gradient in the water. A comparison of the data with model calculations is shown in Figure 17. The results for a range of 10 km are shown at the bottom. The starred point on the calculated curve marks the estimated cut-off frequency. Again, the sound speed ratio at the bottom was not known and a value of $C_2/C_1 = 1.03$ was assumed. Unfortunately, data at frequencies below 200 Hz were not available at this range but a transition between water-duct and no water-duct propagation loss in the vicinity of the cut-off frequency would not require any unreasonable gyrations of the transmission loss vs range curve. On the other hand, data and calculations for a range of 100 km (top) do not appear to be consistent with the model in that the calculated loss appears to be far too low. In the model calculations, 99% of the energy reaching a range of 100 km left the source with vertical angles between zero and 2.2° . This compares with angles of entry between zero and 8.0° for 99% of the energy at a range of 10 km. If, for example, rays were prohibited from entering the sediments at angles less than 2.6° , the model would underestimate the loss by about 4.6 dB at 10 km and 26 dB at 100 km. This is a possible source of error in the simple model used here. If the environmental conditions depart radically from those assumed in the idealized model, significant errors might be incurred. Such environmental departures might include such things as changes in the sediment structure either horizontally or vertically, topographic features in the sea-bed, or strong perturbations in the sound speed profile. Perturbations in the environment occurring in scales which are smaller than a wave-length cannot be handled by simple ray theory. On the other hand, the use of more sophisticated wave-theory models would usually not be justified since environmental parameters are seldom known in great detail. The results obtained using our simple model should be

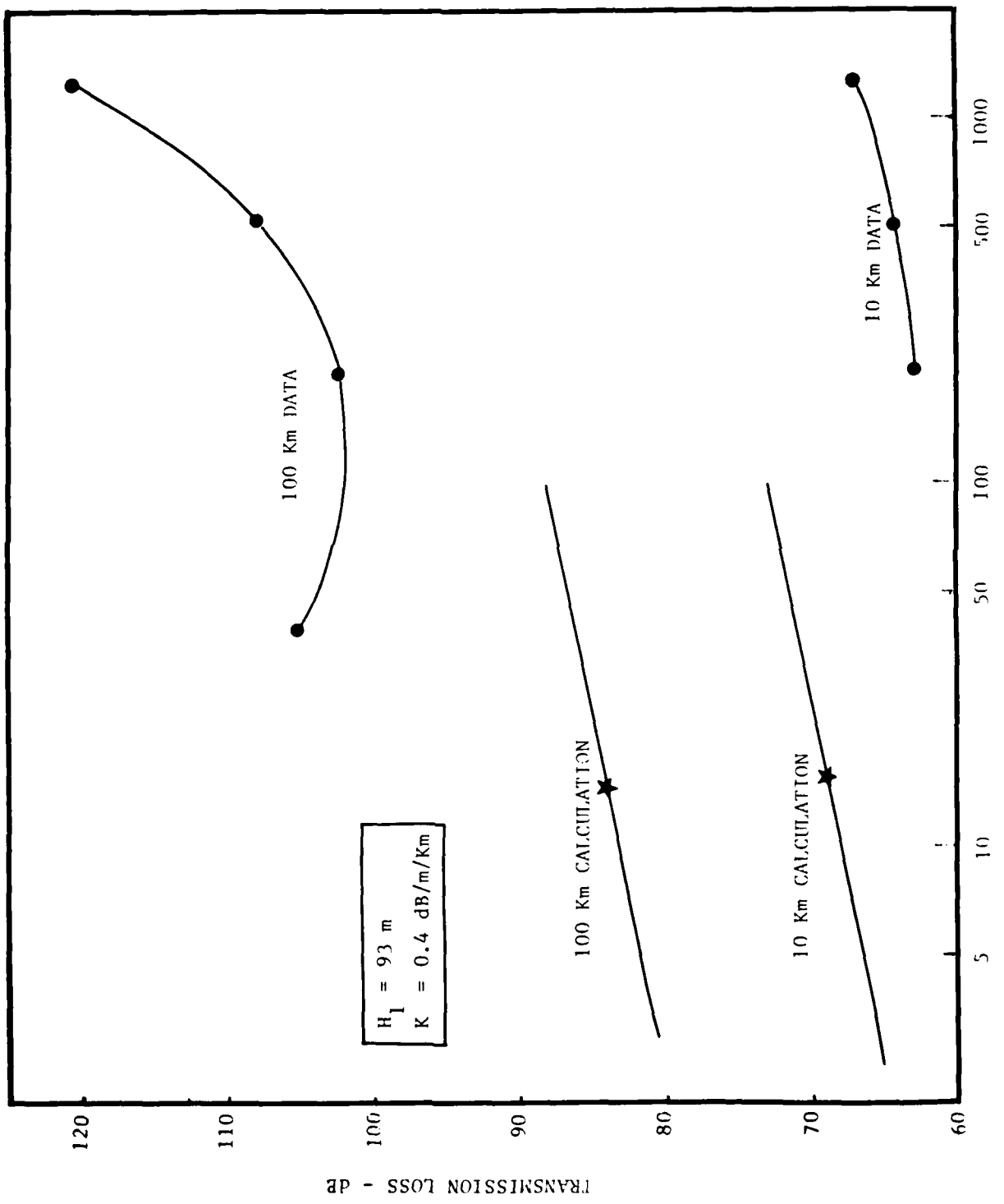


Figure 17. Transmission loss data taken under environmental conditions departing strongly from those assumed in the model

interpreted as being indicative of sensitivity to major parameters and quantitatively predictive only in simple, idealized environments. Since perturbations in the environment would most likely increase the loss, model predictions could be interpreted as meaning the losses can be as low as those predicted.

Although the detailed structure of sediments is seldom known, the sound speed profile in the water can be measured readily, at least in a few sample locations and time. Therefore, a wave theory study on the effects of profile in the water on no water-duct propagation would be useful.

Data sets which include measurements at very low frequencies are rare. One such data set was recently reported by Hecht¹¹. The measurements were made in an area South of Martha's Vinyard. Two sets of measurements were made along an East-West track having a nearly constant water depth of 55 m. Explosive charges were used as sound sources and the data was processed in 1/3 octave bands for frequencies ranging from 8 to 200 Hz. Transmission loss measured at a hydrophone position 0.4 m above the bottom is examined here for comparison with model calculations. For each frequency band we took the mean value (linear power average) of all datum points falling in the range bins of 8 to 12 and 16 to 24 km, combining the data from both runs. The number of datum points at each frequency and the spread in loss values are given in Table I. The results are shown in Figure 18 where the mean values of transmission loss are plotted as a function of frequency for each of two ranges, 10 and 20 km. Results of model calculations are shown for comparison. Environmental inputs used in the model were a water depth of 55 m, sediment layer thickness of 655 m, and an assumed value of 0.4 dB/m/kHz for the attenuation coefficient of the sediments. The cut-off frequency of 12.6 Hz was estimated using a water sound speed at the bottom of 1490 m/sec (from sound speed profile) and sound speed in the sediment of 1800 m/sec. The sediment thickness and the sound speed in the sediment were those given by Hecht as having been determined by standard seismic refraction techniques reported by Ewing et al¹². Losses calculated by the model are shown as a solid line for frequencies from 3 Hz to 12.6 Hz (cut-off frequency), and by a dashed line for higher frequencies.

TABLE I

Frequency - Hz	No. of Data Points		Spread in TL Values - dB	
	10 Km	20 Km	10 Km	25 Km
8	5	8	17.5	25.0
10	9	5	23.0	6.9
12.5	10	11	4.5	14.4
16	10	10	4.5	7.5
20	10	11	3.5	11.0
25	10	12	7.0	9.7
31.5	10	11	6.0	9.6
40	11	11	6.0	12.6
50	10	11	9.0	16.9
63	10	11	9.0	15.3
80	10	11	12.0	14.3
100	10	11	14.8	13.0
125	10	11	7.7	13.1
160	10	11	14.3	15.0
200	10	11	15.9	12.2

Data from two runs along an East-West track at a site South of Martha's Vineyard were examined in the range increments 8 to 12 km and 16 to 24 km. The mean value of the loss within each increment was taken as the loss value at ranges of 10 and 20 km respectively. The first column designates the 1/3 octave frequency band. The second and third columns give the number of datum points averaged in each of two range increments. The fourth and fifth columns show differences between the highest and lowest values of transmission loss in each increment.

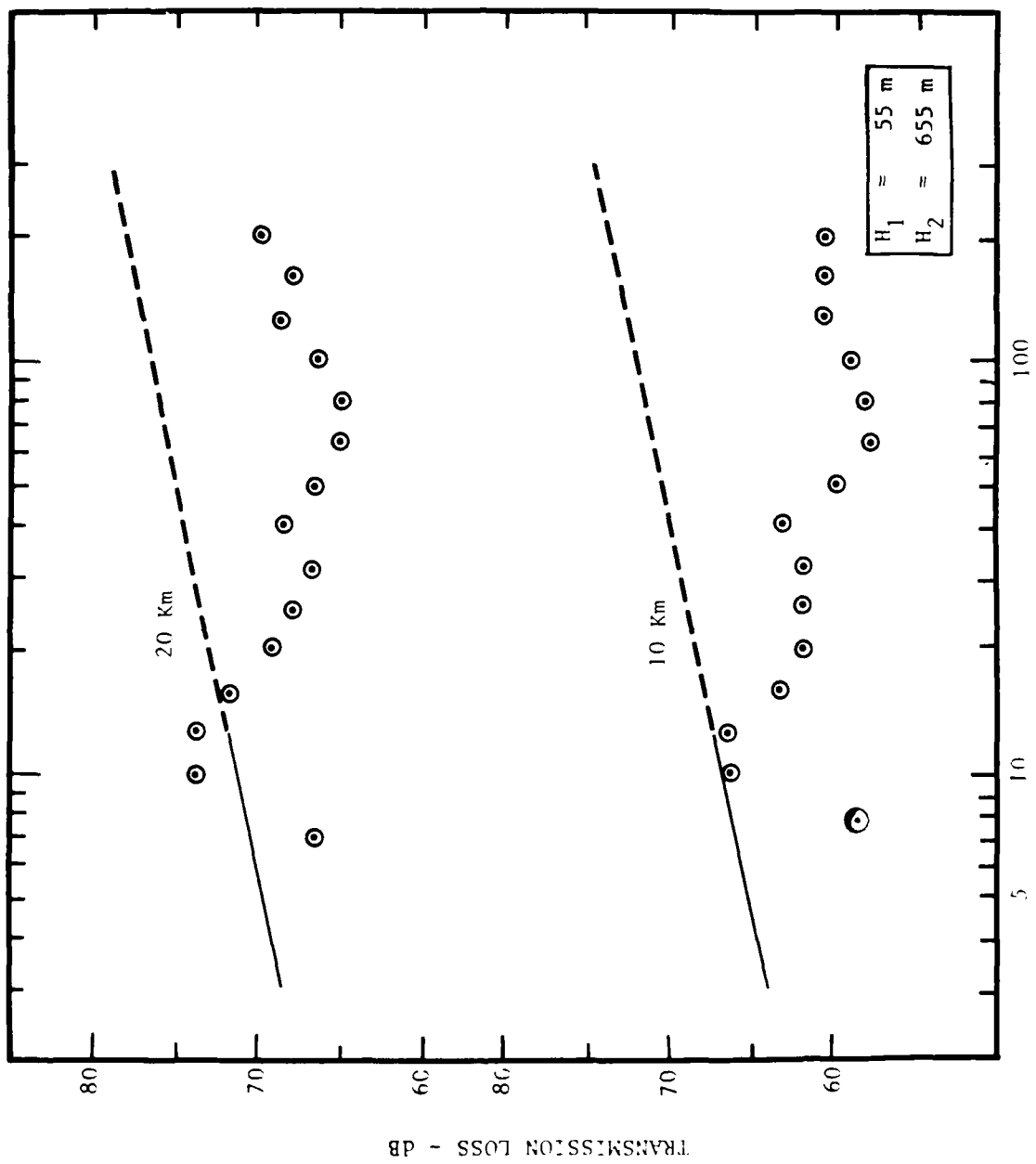


Figure 18. Comparison of model predictions with low-frequency transmission loss data measured in an area South of Martha's Vineyard (Hecht).

Measured transmission loss at 10 and 12.6 Hz agree well with the predicted values for below cut-off propagation. At 20 km the model predicts a lower loss than the measurements (again at 10 and 12.6 Hz) by about 2 dB. Although this is probably a negligible discrepancy considering the scatter of the data and the simplicity of the model, it might be that the model is in error, predicting too low a loss, because of the model assumption of isovelocity water. The actual sound speed profile was strongly downward refracting with an average gradient of about - 0.6 m/sec/m. The possible effect of this was explained earlier in the discussion of the previous illustration. Above cut-off, the loss decreases and then passes through a minimum as expected.

A puzzling feature is the low value of loss at 8 Hz. When the entire data set is examined it appears that the 7 to 8 dB difference in loss between 8 and 10 Hz is statistically significant. All of the data from the two runs along the East-West track at 8 and at 10 Hz are plotted in Figure 19. At least for ranges greater than 5 km the difference in loss between the two frequencies is obvious. Unless the source level for the explosive charges was grossly different from the value used, the decrease in loss at 8 Hz is significant and unexplained by the methods of this study.

CONCLUSIONS

At frequencies below cut-off, for the assumed environmental model, all rays in the propagating field have part of their path lengths in the sediments where they are absorbed at rates ranging from 0.06 to 0.75 dB/m/KHz depending on sediment type. Since most of the energy contributing to the field at long ranges is carried by rays which do not penetrate deeply into the sediments (they have a smaller proportion of their lengths in the sediment), the energy is concentrated in the water column and in the uppermost part of the sediment layer. The following conclusions apply to a sensor located at a depth near the water-sediment interface.

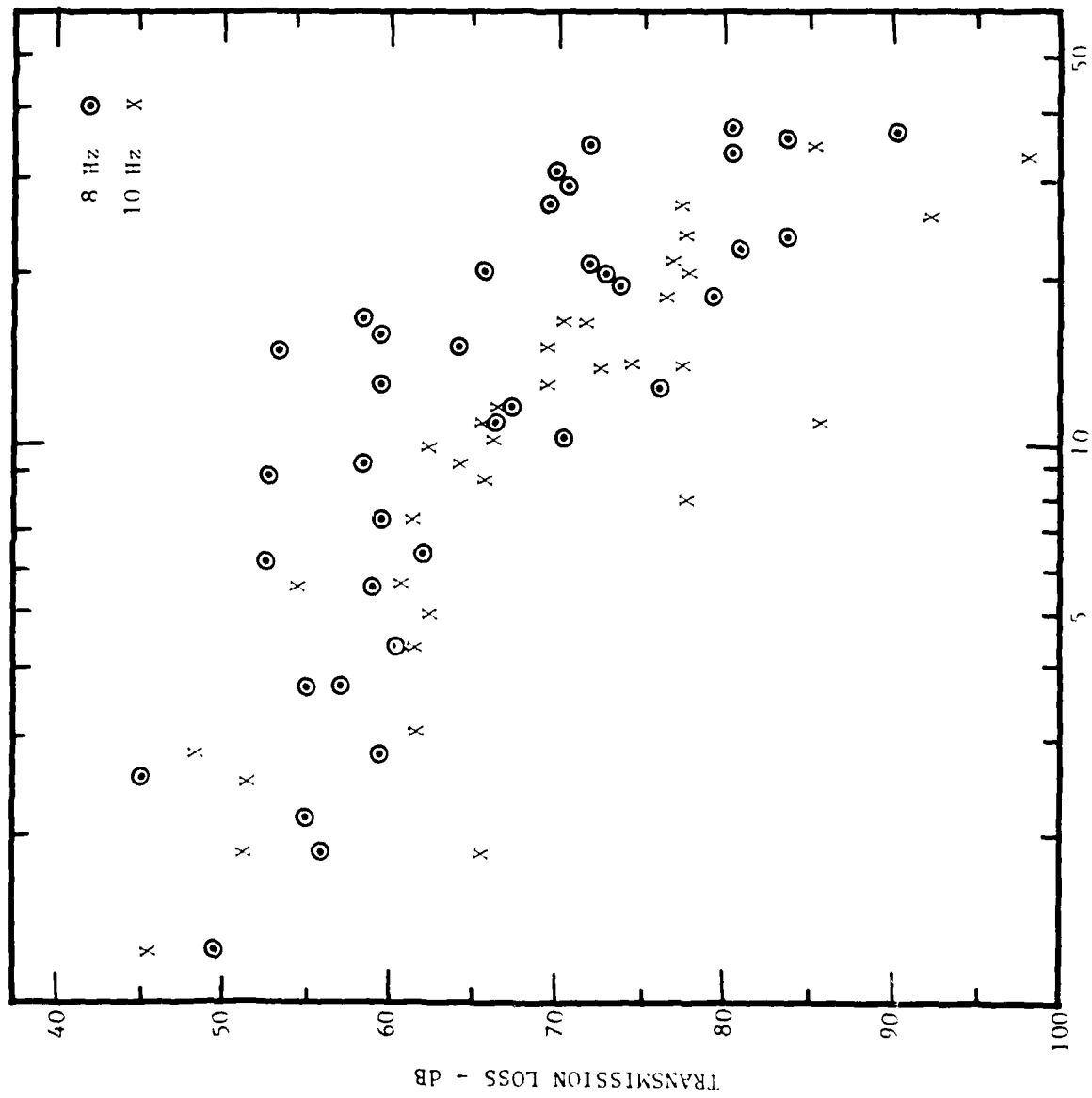


Figure 19. Comparison of 8 Hz and 10 Hz transmission loss data from an area south of Martha's Vineyard (Hecht). The 7 to 8 dB reduction in loss at 8 Hz is unexplained by the model.

Transmission losses, at frequencies below cut-off, are comparable with losses in a water-duct at frequencies of a few hundred Hz. In below cut-off propagation, however, the loss is controlled predominantly by the width of the vertical angle sector of rays which contribute significantly to the field. The result of this is that, at long ranges (greater than a few tens of km), the dependence of loss on range is quite different from that seen in propagation at frequencies above cut-off. Below cut-off, at long ranges, the rate of loss increase (expressed in dB) is approximately proportional to $\log R$, whereas, above cut-off, it tends to become proportional to R . This reduces the "myopic" effect occurring at higher frequencies in shallow water, where detection ranges of targets (or interfering noise sources) are truncated rather abruptly. While this appears to be an advantage for long range detection, it might prove to be a disadvantage for moderate range detection in areas of heavy shipping since "myopic propagation" tends to shield a sensor from distant shipping noise. The manner in which loss, below cut-off, is largely controlled by ray-stripping, also tends to reduce the sensitivity of loss to changes in frequency and to the attenuation coefficients of the sediments.

The results obtained with the idealized model disclose major trends and sensitivity to gross environmental parameters. Quantitative prediction of transmission loss apply only in environments consistent with the model. If there are perturbations in the environment which are not accommodated by the model, errors in predicted values of loss might be expected. Such environmental departures might include such things as spatially varying sediment structure either in range or depth, topographic features in the sea-bed, or strong perturbations in the sound speed profile. Perturbations in the environment occurring in scales smaller than a wavelength cannot be handled by simple ray theory. On the other hand, the use of more sophisticated wave-theory models for more accurate prediction cannot usually be justified since environmental parameters are seldom known in detail. Other than for site-specific prediction, however, wave-theory

models could be usefully employed to study the generic effects of small scale perturbations such as in the sound speed profile. Since variations in the environment would, in most cases, tend to increase the loss, model predictions should be interpreted as meaning that the losses can be as low as those predicted.

The following are specific conclusions regarding shallow water propagation at frequencies below cut-off. Those referring to transmission loss assume a sensor in the water column.

- With respect to depth, intensity is a maximum in the water column (where it is constant with depth). Below the water-sediment interface the intensity decreases rapidly with depth and the rate of decrease increases with range, frequency, and the coefficient of attenuation in the sediments.
- Transmission loss increases with water depth at a rate of approximately 1.5 dB per depth doubled, being approximately 5 dB higher for a water depth of 500 m than for a water depth of 50 m.
- Transmission loss increases with increasing coefficient of attenuation in the sediments. Over the expected range of values of the coefficient, 0.06 to 0.75 db/m/KHz, the loss increases approximately 1.5 dB per doubling of the value of the coefficient.
- Transmission loss increases with frequency at an approximate rate of 1.5 dB per frequency doubled.
- Transmission loss increases with range at a rate of approximately 4.5 dB per range doubled. At long ranges this characteristic differs significantly from that for frequencies above cut-off where the loss increase (expressed in dB) is nearly proportional to R rather than $\log R$.
- The thickness of the sediment layer has only a marginal effect on transmission loss for the range of thickness considered (50 to 1000m).

- Transmission loss at frequencies below cut-off is comparable (not hugely greater or less) with that for ducted propagation at a few hundred Hz.
- In general, as frequency is increased past cut-off, transmission loss can be expected to decrease as the energy becomes trapped in the water-duct.
- A comparison with one data set which extended to frequencies below cut-off showed good agreement with transmission less predicted by the ray-trace model.

Acoustic propagation in shallow water at frequencies below the cut-off of the duct does not appear to be inherently degraded relative to frequencies above cut-off. The performance of systems at very low frequencies is not apt to be defeated by high transmission loss. On the other hand, very low frequencies do not offer any obviously marked advantage here. An assessment of relative system performance must hinge on a combined evaluation of all major factors in passive system performance including transmission loss, ambient noise, self noise, target radiation, and limitations on temporal and spatial signal processing. Such an evaluation is recommended.

REFERENCES

1. Pekeris, C.L., "Theory of Propagation of Explosive Sound in Shallow Water", Geol. Soc. Am. Memo 27, 1948
2. Ferris, R.H., "Characterization of Transmission Loss for Performance Prediction in Shallow Water", MAR, Incorporated Technical Note 150, October 1980
3. Brekhovskikh, L.M., "Waves in Layered Media", Academic Press, Incorporated, New York, 1960
4. Hamilton, E.L., "Compressional Wave Attenuation in Marine Sediments", Geophysics, Volume 37, No. 4, August 1972, P. 620-646
5. Hamilton, E.L., "Geoacoustic Models of the Sea Floor", published in "Physics of Sound in Marine Sediments", Plenum Press, New York, edited by Loyd Hampton, 1974
6. Houtz, R.E., and Ewing, J.I., "Sediment Velocities of the Western North Atlantic Margin", Bull. of the Seismological Soc. Am., Volume 54, No. 3, PP. 867-895
7. Hamilton, E.L., "Sound Velocity Gradients in Marine Sediments", J. Acous. Soc. Am. 65 (4), April 1979, PP. 909-922
8. Hanna, J.S., "Short Range Transmission Loss and the Evidence for Bottom Refracted Energy", J. Acous. Soc. Am. 53, PP. 1686-1690
9. Urick, R.J., "Principles of Underwater Sound", 2nd edition, McGraw Hill Book Company, New York, 1975
10. Ross, J.M. and Adlington, R.H., "Acoustic Propagation Loss and Noise Measurements on the Canadian Eastern Continental Shelf", DREA Research Note SA/76/9, 1976, Informal Communication
11. Hecht, R.J., "Sound Propagation South of Martha's Vineyard", Underwater Systems, Incorporated report prepared for office of Naval Research Code 464, June 1980
12. Ewing, M., Werzel, J.L., Steenland, H.C. and F. Press, "Geophysical Investigations in the Emerged and Submerged Atlantic Coastal Plain", Bull. Geol. Soc. Am., Volume 61, September 1950, P. 877

APPENDIX A

Derivation of Transmission Loss Equations

The source, located in the water, is assumed to be omnidirectional with an intensity at one meter of I_0 . Ray tracing will be done for rays leaving the source at 2° increments in the vertical starting at 1° (for calculations at very long ranges, the increment used is 0.2°). A ray at angle θ is assumed to carry the power radiated in the interval $\theta \pm 1^\circ$, i.e., that crossing the shaded area in Figure A-1. The power in each 2° segment, $\Delta p(\theta)$, is given by:

$$\Delta p(\theta) = 2I_0 \Delta A(\theta) = 8\pi I_0 \sin 1^\circ \cos \theta = 0.4386 I_0 \cos \theta, \quad (A-1)$$

where $\Delta A(\theta)$ is the area on the surface of a sphere of radius 1m between the vertical angles of $\theta \pm 1^\circ$. The area is doubled to account for both upward and downward going rays.

At range R (the horizontal distance to a field point, measured radially from the source), the acoustic field, with the exception of that part which has penetrated the sediment basement interface, is confined between the water's surface and the bottom of the sediment layer. When R is large compared to $H_1 + H_2$, the field will be distributed over an area given approximately by the area of a right, circular cylinder of radius R and height $H_1 + H_2$, i.e., $2\pi R (H_1 + H_2)$. Several types of ray paths are shown in Figure A-2 (not drawn to scale). The two shallowest angles are a pair of upward and downward going rays which are refracted upward before reaching the basement. The ray at the next steeper angle is one of a pair (upward going ray not shown) which are reflected from the basement. The steepest ray reaches the basement at an angle greater than critical and is lost. One complete cycle is shown for each ray which returns to the water column. At the end of a cycle the ray has returned to the initial condition it had on leaving the source. From that point, the ray path will be repeated as range is increased. The cycle length, e.g., the horizontal

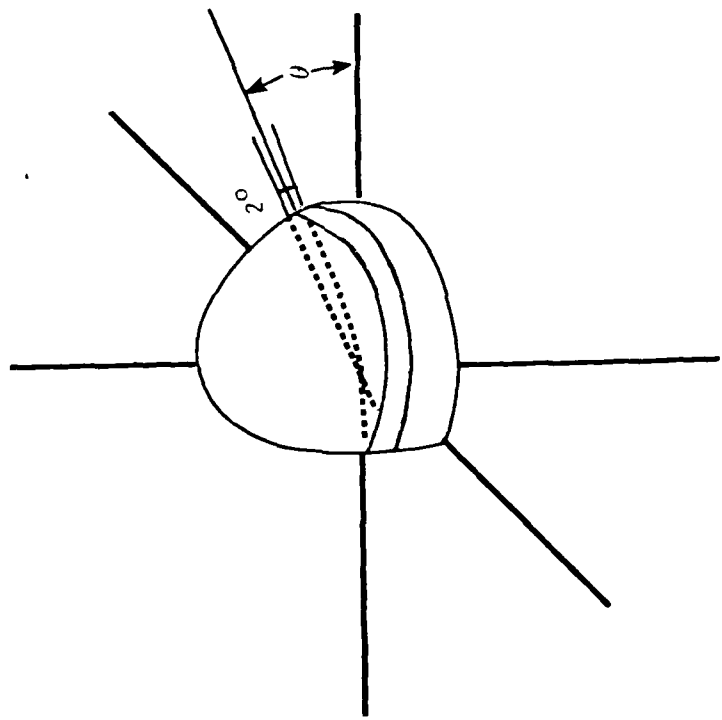


Figure A-1. Diagram showing annular strip on a sphere of unit radius about a point acoustic source at the origin. The power crossing the annular strip is assigned to the ray which bisects the strip at vertical angle θ .

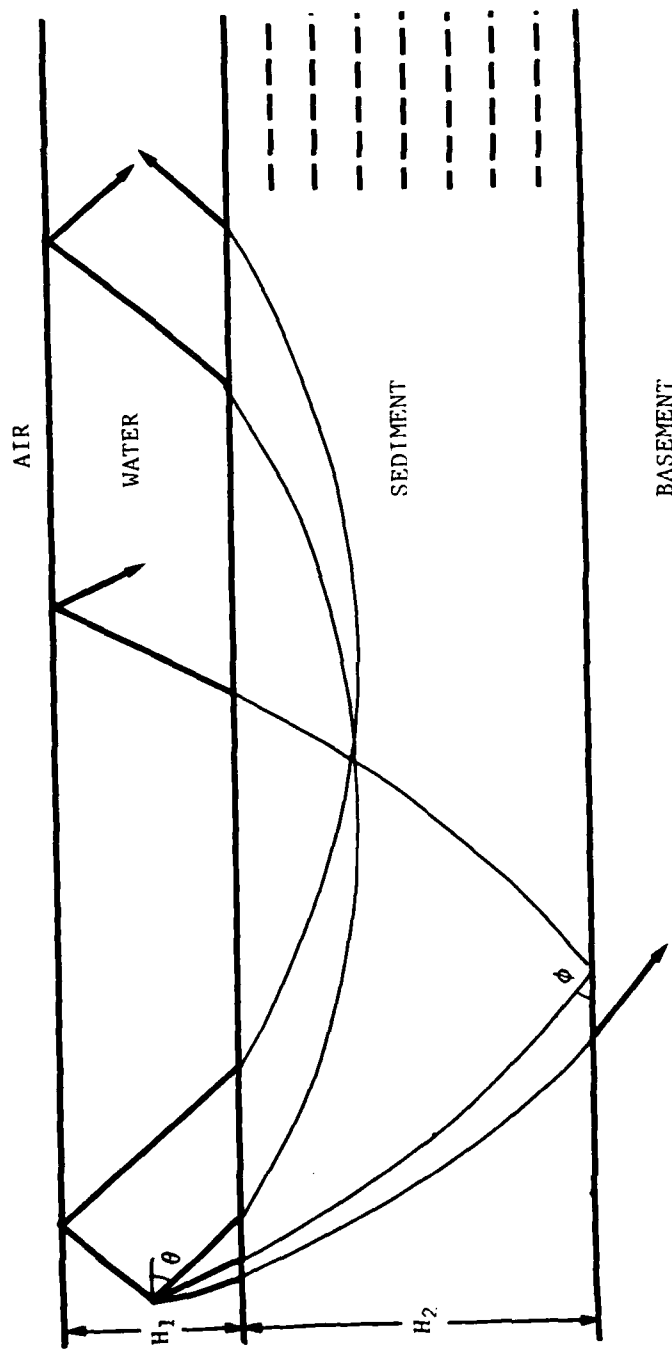


Figure A-2. Examples of types of ray paths occurring with the model geometry shown in Figure 5 of the text. All rays penetrate the water-sediment interface. For small values of θ , the rays are refracted upward before reaching the basement. Rays leaving the source at larger values of θ (up to 68°) are reflected from the sediment-basement interface. Rays leaving the source reflected from the sediment-basement interface. Rays leaving the source at angles greater than 68° penetrate the basement. Arbitrary division of the sediment into depth increments is shown by the dashed lines at the right.

advance of the ray in one cycle, is a function of the vertical angle at which the ray left the source. The sediment is divided into arbitrary layers as shown by the dashed lines at the right. Within a layer, at range R , the field is assumed to be uniformly distributed over the surface area of a right circular cylinder of radius R and height H_n where H_n is the thickness of the layer. In the water column the field (intensity but not pressure) is distributed uniformly over the surface of a cylinder of radius R and height H_1 . We will determine the average intensity in each layer as a function of range by summing the power carried by all rays within the layer and dividing by the area of the cylinder. Since we are concerned with the flow of power normal to the cylinder's surface we should, strictly, sum the powers of the horizontal components of the rays. In this model, however, since almost all of the power is carried by rays of angle less than 30° (see Figure 11 in the text) we make the approximation of summing the total ray powers.

The ray paths in the water are straight lines and the paths in the sediment are arcs of circles of radius r given by:

$$r = \frac{1500}{g \cos \theta} \quad (A-2)$$

The centers of the circles lie at a depth where c would equal zero if the gradient was continued upward. If the ray is not refracted upward before reaching the sediment-basement interface, it encounters the interface at grazing angle ϕ given by:

$$\phi = \cos^{-1} \left[\left(1 + \frac{gH_2}{1500} \right) \cos \theta \right] \quad (A-3)$$

The critical angle, θ_c , at this interface is given by:

$$\theta_c = \cos^{-1} \frac{c_1}{c_2} = \cos^{-1} \left(\frac{1500 + gH_2}{4000} \right) \quad (A-4)$$

Referring to Figure A-3 we see that ϕ is related to θ by:

$$\cos \phi = \left(1 + \frac{gH_2}{1500} \right) \cos \theta \quad (A-5)$$

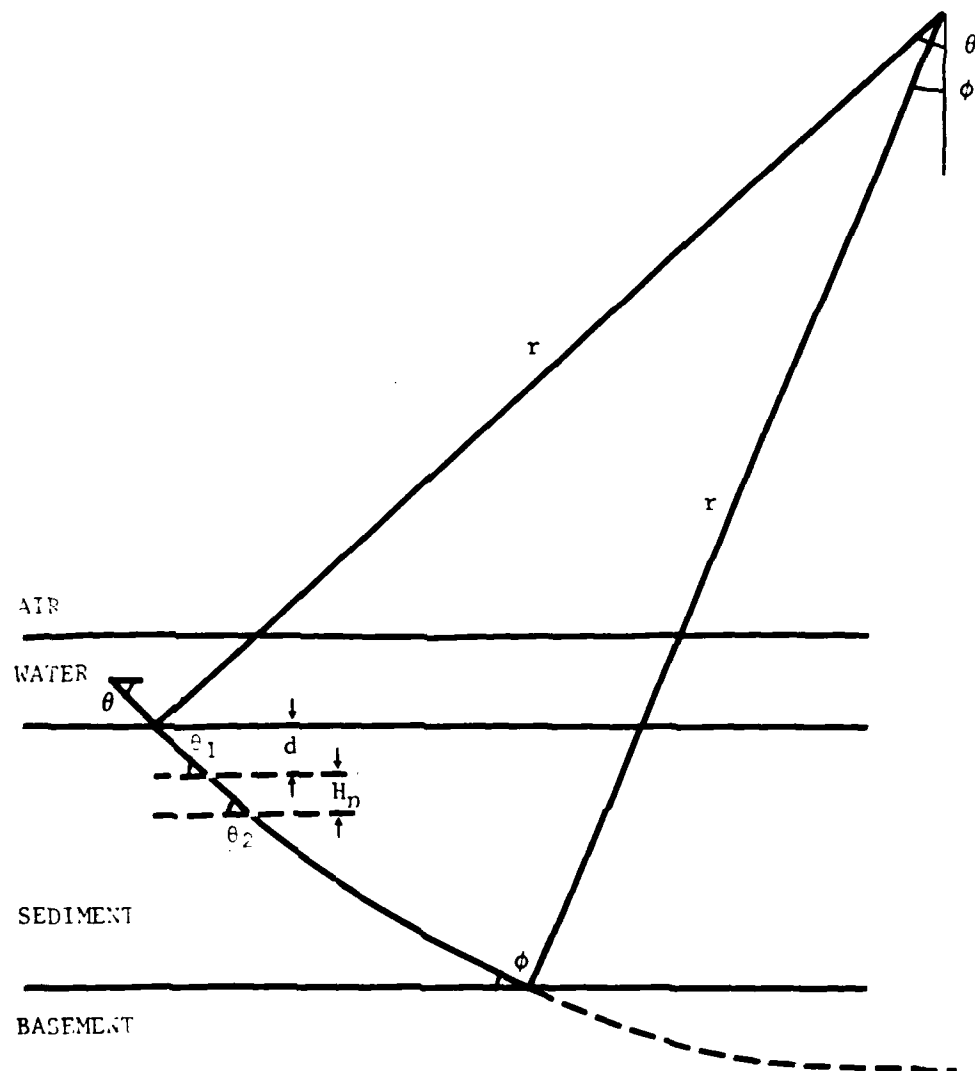


Figure A-3. Diagram defining the angles θ , θ_1 , θ_2 , and ϕ . Rays is the sediment are refracted along the area of a circle of radius r . A ray leaving the source at angle θ intercepts the upper boundary of the n th layer at angle θ_1 , the lower boundary at angle θ_2 , and the basement at angle ϕ .

The value of θ associated with φ_c is then given by:

$$\theta = \cos^{-1} \left[\frac{1500}{1500 + gH_2} \cdot \frac{1500 + gH_2}{4000} \right] = 68^\circ \quad (A-6)$$

Therefore, only these rays between $\pm 1^\circ$ and $\pm 67^\circ$ will contribute to the long-range field and this is independent of the value of H_2 .

In summing the rays in any given layer we wish to average out the small scale fluctuations with range that occur within a cycle length. To do this we take the contribution of each ray as being proportional to the probability of finding that ray within the designated depth increment. This probability, $P(n, \theta)$, is equal to the ratio of the horizontal advance within the designated depth increment per cycle to the total horizontal advance per cycle. Also, the attenuation of a ray is taken to be proportional to the ratio of the path length in the sediment per cycle to the horizontal advance per cycle, PL/RA . Using these procedures we now can calculate the power, intensity, and, finally, the transmission loss in each layer as a function of range.

The power for each ray at range, R , is given by:

$$p(\theta, R) = \left(10^{-0.1 KfR \frac{PL}{RA}} \right) 0.4386 I_0 \cos \theta, \quad (A-7)$$

where K is the attenuation coefficient of the sediment in dB/m/kHz, f is the frequency in kHz, and R is the horizontal range from the source. The average power in the n th layer is given by:

$$p(n, R) = 0.4386 I_0 \sum_{\theta=1}^{67} \left(10^{-0.1 KfR \frac{PL}{RA}} \right) P(n, \theta) \cos \theta, \quad (A-8)$$

where θ takes on odd integer values in the range from 1 to 67. The average intensity in the n th layer is given by:

$$I_n = \frac{0.4386}{2\pi R H_n} \sum_{\theta=1}^{67} \left(10^{-0.1 KfR \frac{PL}{RA}} \right) P(n, \theta) \cos \theta, \quad (A-9)$$

where H_n is the thickness of the n th layer. Finally, the transmission loss at range R in the n th layer is given by:

$$TL(R, n) = 10 \log I_o - 10 \log I_n = -10 \log \left[\frac{1}{14.3 RH_n} \sum_{\theta=1}^{67} \left(10^{-0.1 KfR} \frac{PL}{RA} \right) P(n, \theta) \cos \theta \right] \quad (A-10)$$

It remains to obtain expressions for $\frac{PL}{RA}$ and $P(n, \theta)$. For rays that reach the basement, the path length in the sediment for one cycle is given by:

$$PL = \frac{\theta - \phi}{360} \cdot 4\pi r = \frac{52.36 (\theta - \phi)}{g \cos \theta} \quad (A-11)$$

If the ray does not reach the basement, ϕ is taken as zero. The range advance per cycle is the sum of the range advance in the water plus the advance in the sediment and is given by:

$$RA = \frac{2H_1}{\tan \theta} + \frac{3000}{g \cos \theta} (\sin \theta - \sin \phi) \quad (A-12)$$

Again, if the ray does not reach the basement, ϕ is taken as zero. Dividing (11A) by (12A) we get:

$$\frac{PL}{RA} = \frac{26.18 (\theta - \phi) \tan \theta}{H_1 g \cos \theta + 1500 (\sin \theta - \sin \phi) \tan \theta} \quad (A-13)$$

As shown in Figure A-3, a ray in the sediment makes angles of θ_1 and θ_2 with the upper and lower boundaries of the n th layer in the sediment. The angles are given by:

$$\theta_1 = \cos^{-1} \left[\left(1 + \frac{gd}{1500} \right) \cos \theta \right], \quad \theta_2 = \cos^{-1} \left[\left(1 + \frac{g(d + H_n)}{1500} \right) \cos \theta \right], \quad (A-14)$$

where d is the depth of the upper boundary of the layer below the water-sediment interface. The probability that the ray will be found in that depth interval is equal to the ratio of the horizontal advance in the interval to the total horizontal advance per cycle. It is given by:

$$P(n, \theta) = \frac{\frac{1500}{g \cos \theta} (\sin \theta_1 - \sin \theta_2)}{\frac{H_1}{\tan \theta} + \frac{1500}{g \cos \theta} (\sin \theta - \sin \phi)} \quad (A-15)$$

when calculating transmission loss to a point in the water layer, $P(n, \theta)$, must be replaced by $P_w(\theta)$, the probability of finding the ray in the water. It is equal to the ratio of the horizontal advance in the water to the total horizontal advance per cycle and is given by:

$$P_w(\theta) = \frac{\frac{H_1}{\tan \theta}}{\frac{H_1}{\tan \theta} + \frac{1500}{g \cos \theta} (\sin \theta - \sin \phi)} \quad (A-16)$$

Transmission loss as a function of range and depth can now be calculated using equations 5A, 10A and 13A through 16A.

DISTRIBUTION LIST

	<u>No. of Copies</u>
Scientific Officer Director Earth and Environmental Physics Program Arctic and Earth Sciences Division Office of Naval Research 800 North Quincy Street Arlington, VA 22217 Attn: Mr. Robert F. Obrochta, Code 464	1
Administrative Contracting Officer Defense Contract Administration Services Management Area-Baltimore 300 East Joppa Road Hampton Plaza Bldg., Room 200 Towson, MD 21204	1
Naval Research Laboratory Washington, DC 20375 Attn: Code 5120 Code 2627	1 6
Defense Technical Information Center Bldg. 5, Cameron Station Alexandria, VA 22314	12
Pennsylvania State University Applied Research Laboratory P.O. Box 30 State College, PA 16801 Attn: Dr. S. McDaniel	1
University of Texas Applied Research Laboratories P.O. Box 8029 Austin, TX 78712 Attn: Dr. K. Hawker	1
University of Texas at Galveston Marine Science Institute Galveston, TX 77550 Attn: Dr. D. McCowan	1
University of Hawaii Hawaii Institute of Geophysics 2525 Correa Road Honolulu, HI 96822 Attn: Dr. T. Brocher	1
Naval Postgraduate School Monterey, CA 93940 Attn: Dept. of Physics and Chemistry Dr. J. Saunders	1

DISTRIBUTION LIST (cont.)

Lamont-Doherty Geological Observatory of Columbia University Palisades, NY 10964	1
Naval Oceanographic Office NSTL Station Bay St. Louis, MS 39522 Attn: Code 7300	1
Ocean/Seismic/Survey, Incorporated 80 Oak Street Norwood, NJ 07648	1
Office of Naval Research Detachment NSTL Station Bay St. Louis, MS 39522 Attn: Code 483	1
Office of Naval Research Eastern Central Regional Office Bldg. 114, Section D 666 Summer Street Boston, MA 02210	1

DAI
FILM